



THE UNIVERSITY *of* EDINBURGH

Edinburgh Research Explorer

## Predictable Properties of Fitness Landscapes Induced by Adaptational Tradeoffs

**Citation for published version:**

Das, SG, Oliveira Lebre Direito, S, Waclaw, B, Allen, R & Krug, J 2020, 'Predictable Properties of Fitness Landscapes Induced by Adaptational Tradeoffs', *eLIFE*, vol. 9, e55155. <https://doi.org/10.7554/eLife.55155>

**Digital Object Identifier (DOI):**

[10.7554/eLife.55155](https://doi.org/10.7554/eLife.55155)

**Link:**

[Link to publication record in Edinburgh Research Explorer](#)

**Document Version:**

Peer reviewed version

**Published In:**

eLIFE

**General rights**

Copyright for the publications made accessible via the Edinburgh Research Explorer is retained by the author(s) and / or other copyright owners and it is a condition of accessing these publications that users recognise and abide by the legal requirements associated with these rights.

**Take down policy**

The University of Edinburgh has made every reasonable effort to ensure that Edinburgh Research Explorer content complies with UK legislation. If you believe that the public display of this file breaches copyright please contact [openaccess@ed.ac.uk](mailto:openaccess@ed.ac.uk) providing details, and we will remove access to the work immediately and investigate your claim.



# Predictable Properties of Fitness Landscapes Induced by Adaptational Tradeoffs

Suman G. Das<sup>1\*</sup>, Susana O. L. Direito<sup>2</sup>, Bartłomiej Waclaw<sup>2</sup>, Rosalind J. Allen<sup>2</sup>, Joachim Krug<sup>1\*</sup>

\*For correspondence:  
sdas3@uni-koeln.de (SGD);  
jkrug@uni-koeln.de (JK)

<sup>1</sup>Institute for Biological Physics, University of Cologne, Cologne, Germany; <sup>2</sup>School of Physics and Astronomy, University of Edinburgh, Edinburgh, United Kingdom

**Abstract** Fitness effects of mutations depend on environmental parameters. For example, mutations that increase fitness of bacteria at high antibiotic concentration often decrease fitness in the absence of antibiotic, exemplifying a tradeoff between adaptation to environmental extremes. We develop a mathematical model for fitness landscapes generated by such tradeoffs, based on experiments that determine the antibiotic dose-response curves of *Escherichia coli* strains, and previous observations on antibiotic resistance mutations. Our model generates a succession of landscapes with predictable properties as antibiotic concentration is varied. The landscape is nearly smooth at low and high concentrations, but the tradeoff induces a high ruggedness at intermediate antibiotic concentrations. Despite this high ruggedness, however, all the fitness maxima in the landscapes are evolutionarily accessible from the wild type. This implies that selection for antibiotic resistance in multiple mutational steps is relatively facile despite the complexity of the underlying landscape.

## Introduction

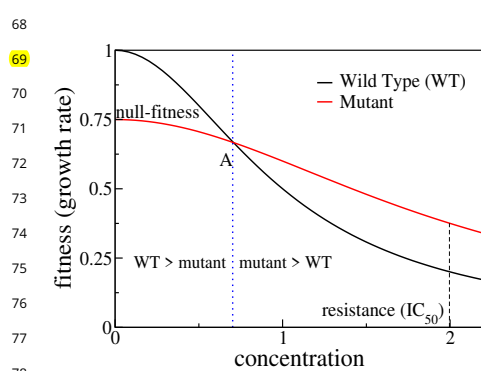
Sewall Wright introduced the concept of fitness landscapes in 1932 (*Wright, 1932*), and for decades afterwards it persisted chiefly as a metaphor, due to lack of sufficient data. This has changed considerably in recent decades (*de Visser and Krug, 2014; Hartl, 2014; Kondrashov and Kondrashov, 2015; Fragata et al., 2019*). There are now a large number of experimental studies that have constructed fitness landscapes for combinatorial sets of mutations relevant to particular phenotypes, such as the resistance of **microbial pathogens** to antibiotics (*Weinreich et al., 2006; DePristo et al., 2007; Marcusson et al., 2009; Lozovsky et al., 2009; Brown et al., 2010; Schenk et al., 2013; Goulart et al., 2013; Mira et al., 2015; Palmer et al., 2015; Knopp and Andersson, 2018*), and the genomic scale of these investigations is rapidly growing (*Wu et al., 2016; Bank et al., 2016; Domingo et al., 2018; Pokusaeva et al., 2019*). Mathematical modeling of fitness landscapes has also seen a revival, motivated partly by the need to quantify and interpret the ruggedness of empirical fitness landscapes (*Szendro et al., 2013; Weinreich et al., 2013; Neidhart et al., 2014; Ferretti et al., 2016; Blanquart and Bataillon, 2016; Crona et al., 2017; Hwang et al., 2018; Kaznatcheev, 2019; Crona, 2020*). Conceptual breakthroughs, such as the notion of sign epistasis (where a mutation is beneficial in some genetic backgrounds but deleterious in others), have shed light on how ruggedness can constrain evolutionary trajectories (*Weinreich et al., 2005; Poelwijk et al., 2007, 2011; Franke et al., 2011; Lobkovsky and Koonin, 2012; Zagorski et al., 2016*).

Despite this progress, a limitation of current studies of fitness landscapes is that they focus

41 mostly on  $G \times G$  (gene-gene) interactions, and little on  $G \times G \times E$  (where  $E$  stands for environment)  
 42 interactions, i.e on how changes in environment modify gene-gene interactions. A few recent  
 43 studies have begun to address this question (Flynn et al., 2013; Taute et al., 2014; Gorter et al.,  
 44 2018; de Vos et al., 2018). In the context of antibiotic resistance, it has been realized that the fitness  
 45 landscape of resistance genes depends quite strongly on antibiotic concentration (Mira et al., 2015;  
 46 Stiffler et al., 2015; Ogbunugafor et al., 2016). This is highly relevant to the clinical problem of  
 47 resistance evolution, since concentration of antibiotics can vary widely in a patient's body as well  
 48 as in various non-clinical settings (Kolpin et al., 2004; Andersson and Hughes, 2014). Controlling  
 49 the evolution of resistance mutants thus requires an understanding of fitness landscapes as a  
 50 function of antibiotic concentration. Empirical investigations of such scenarios are still limited, and  
 51 systematic theoretical work on this question is also lacking.

52 In the present work, we aim to develop a theory of  $G \times G \times E$  interactions for a specific class of  
 53 landscapes, with particular focus on applications to antibiotic resistance. The key feature of the  
 54 landscapes we study is that every mutation comes with a tradeoff between adaptation to the two  
 55 extremes of an environmental parameter. For example, it has been known for some time that  
 56 antibiotic resistance often comes with a fitness cost, such that a bacterium that can tolerate high  
 57 drug concentrations grows slowly in drug-free conditions (Andersson and Hughes, 2010; Melnyk  
 58 et al., 2015). While such tradeoffs are not universal (Hughes and Andersson, 2017; Durão et al.,  
 59 2018), they certainly occur for a large number of mutations and a variety of drugs.

60 Tradeoffs can also arise in complex scenarios involving multiple drugs. It has been reported  
 61 in Stiffler et al. (2015) that certain mutations in TEM-1  $\beta$ -lactamase are neutral at low ampicillin  
 62 concentration but deleterious at high concentration, and that a number of the latter mutations  
 63 also confer resistance to cefotaxime. Therefore in a medium with cefotaxime and a moderately  
 64 high concentration of ampicillin, it is possible that these mutations will be deleterious at low  
 65 cefotaxime concentrations but beneficial at high cefotaxime concentration. Fitness landscapes  
 66 with adaptational tradeoffs are therefore also of potential relevance to evolution in response to  
 67 multi-drug combinations.



70  
 71  
 72  
 73  
 74  
 75  
 76  
 77  
 78  
 79 **Figure 1.** Schematic showing dose response  
 80 curves of a wild type and a mutant. To the left  
 81 of the intersection point A the wild type is  
 82 selected over the mutant, whereas to the right  
 83 of A the mutant is selected.

84  
 85  
 86 swapping the rank order between the two fitness values. The intersection point is known as the  
 87 minimum selective concentration (MSC), and it defines the lower boundary of the mutant selection  
 88 window (MSW) within which the resistance mutant has a selective advantage relative to the wild  
 89 type (Khan et al., 2017; Alexander and MacLean, 2018).

90 When there are several possible mutations and multiple combinatorial mutants, a large number  
 91 of such intersections occur as the concentration of the antibiotic increases. This leads to a succes-

Our starting point for understanding these landscapes is the knowledge of two phenotypes that are well studied – the drug-free growth rate (which we call the null-fitness) and the  $IC_{50}$  (the drug concentration that reduces growth rate by half), which is a measure of antibiotic resistance. These two phenotypes correspond to the two extreme regimes of an environmental parameter, i.e zero and highly inhibitory antibiotic concentrations. The function that describes the growth rate of a bacterium for antibiotic concentrations between these two extremes is called the dose-response curve or the inhibition curve (Regoes et al., 2004). When tradeoffs are present, the dose-response curves of different mutants must intersect as the concentration is varied (Gullberg et al., 2011). This is schematically shown in Figure 1. The intersection of dose-response curves of the wild type and the mutant happen at point A,



92 sion of different fitness landscapes defined over the space of genotype sequences (Maynard Smith,  
 93 1970; Kauffman and Levin, 1987). Whenever the curves of two mutational neighbors (genotypes  
 94 that differ by one mutation) intersect, there can be an alteration in the evolutionary trajectory  
 95 towards resistance, whereby a forward (reverse) mutation now becomes more likely to fix in the  
 96 population than the corresponding reverse (forward) mutation. These intersections change the  
 97 ruggedness of landscapes and the accessibility of fitness maxima. In this way a rich and complex  
 98 structure of selective constraints emerges in the MSW. To explore the evolutionary consequences  
 99 of these constraints, we construct a theoretical model based on existing empirical studies as well  
 100 as our own work on ciprofloxacin resistance in *E. coli*. Specifically, we address two fundamental  
 101 questions: (i) How does the ruggedness of the fitness landscape vary as a function of antibiotic  
 102 concentration? (ii) How accessible are the fitness optima as a function of antibiotic concentration?

103 We find that even when the null-fitness and resistance values of the mutations combine in  
 104 a simple, multiplicative manner, the intersections of the curves produce a highly epistatic land-  
 105 scape at intermediate concentrations of the antibiotic. This is an example of a strong  $G \times G \times E$   
 106 interaction, where changes in the environmental variable drastically alter the interactions between  
 107 genes. Despite the high ruggedness at intermediate concentrations, however, the topology of  
 108 the landscapes is systematically different from the oft-studied random landscape models, such as  
 109 the House-of-Cards model (Kauffman and Levin, 1987; Kingman, 1978), the Kauffman NK model  
 110 (Kauffman and Weinberger, 1989; Hwang et al., 2018) or the Rough Mt. Fuji model (Neidhart et al.,  
 111 2014). For example, most fitness maxima have similar numbers of mutations that depend logarith-  
 112 mically on the antibiotic concentration. Importantly, all the fitness maxima remain highly accessible  
 113 through adaptive paths with sequentially fixing mutations. In particular, any fitness maximum  
 114 (including the global maximum) is accessible from the wild type as long as the wild type is viable. As  
 115 a consequence, the evolution of high levels of antibiotic resistance by multiple mutations (Hughes  
 116 and Andersson, 2017; Wistrand-Yuen et al., 2018; Rehman et al., 2019) is much less constrained by  
 117 the tradeoff-induced epistatic interactions than might have been expected on the basis of existing  
 118 models.

## 119 Results

### 120 Mathematical model of tradeoff-induced fitness landscapes

121 The chief goal of this paper is to develop and explore a mathematical framework to study tradeoff-  
 122 induced fitness landscapes. We consider a total of  $L$  mutations, each of which increases antibiotic  
 123 resistance. A fitness landscape is a real-valued function defined on the set of  $2^L$  genotypes made  
 124 up of all combinations of these mutations. A genotype can be represented by a binary string of  
 125 length  $L$ , where a 1 (0) at each position represents the presence (absence) of a specific mutation.  
 126 Alternatively, any genotype is uniquely identified as a subset of the  $L$  mutations (the wild type is the  
 127 null subset, i.e the subset with no mutations).

128 In this paper, unless mentioned otherwise, we define the fitness  $f$  as the exponential growth  
 129 rate of a microbial population. The fitness is a function of antibiotic concentration. This function has  
 130 two parameters of particular interest to us – the growth rate at zero concentration, which we refer  
 131 to as the null-fitness and denote by  $r$ , and a measure of resistance such as  $IC_{50}$  which we denote  
 132 by  $m$ . Each single mutation is described by the pair  $(r_i, m_i)$ , where  $r_i$  and  $m_i$  are the null-fitness and  
 133 resistance values respectively of the  $i$ th single mutant. We further rescale our units such that for  
 134 the wild type,  $r = 1$  and  $m = 1$ . We consider mutations that come with a fitness-resistance tradeoff,  
 135 i.e a single mutant has an increased resistance ( $m_i > 1$ ) and a reduced null-fitness ( $r_i < 1$ ) compared  
 136 to the wild type. To proceed we need to specify two things: (i) how the fitness of the wild type and  
 137 the mutants depend on antibiotic concentration, and in particular if this dependence exhibits a  
 138 pattern common to various mutant strains; (ii) how the  $r$  and  $m$  values of the combinatorial mutants  
 139 depend on those of the individual mutations. To address these issues we take guidance from two  
 140 empirical observations.

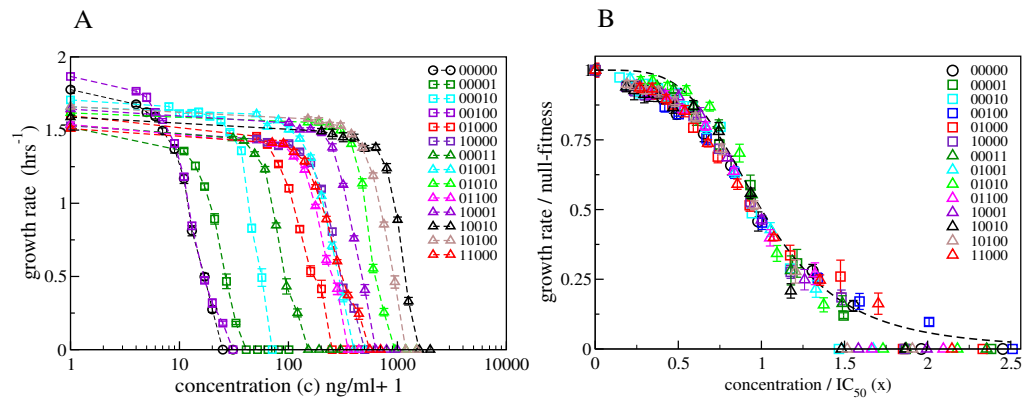


**Figure 2.** Dose-response curves for *E. coli* in the presence of ciprofloxacin. Each binary string corresponds to a strain, where the presence (absence) of a specific mutation in the strain is indicated by a 1(0). The five mutations in order from left to right are S83L (*gyrA*), D87N (*gyrA*), S80I (*parC*),  $\Delta marR$ , and  $\Delta acrR$ . The names of the strains are given in Table 1 in Materials and Methods. **(A)** Dose-response curves of the wild type, the five single mutants and eight double mutants. Unlike the experiments reported in *Marcusson et al. (2009)*, the mutants were grown in isolation rather than in competition with the wild type. **(B)** The same curves, but scaled with the null-fitness and  $IC_{50}$  of each individual genotype. The dashed black line is the Hill function  $(1 + x^4)^{-1}$ .

141 Scaling of dose-response curves

142 *Marcusson et al. (2009)* have constructed a series of *E. coli* strains with single, double and triple  
 143 mutations conferring resistance to the fluoroquinolone antibiotic ciprofloxacin (CIP), which inhibits  
 144 DNA replication (*Drlica et al., 2009*). In their study they measured MIC (minimum inhibitory con-  
 145 centration) values and null-fitness but did not report dose-response curves. Some of the present  
 146 authors have recently shown that the dose-response curve of the wild-type *E. coli* (strain K-12  
 147 MG1655) in the presence of ciprofloxacin can be fitted reasonably well by a Hill function (*Ojkic et al.,*  
 148 **2019**).

149 Here we expand on this work and determine dose-response curves for a range of single- and  
 150 double-mutants with mutations restricted to five specific loci known to confer resistance to CIP  
 151 (*Marcusson et al., 2009*) (see Materials and Methods). Figure 2A shows the measured curves for  
 152 the wild type, the five single mutants, and eight double-mutant combinations. The genotypes are  
 153 represented as binary strings, where a 1 or 0 at each position denotes respectively the presence or  
 154 absence of a particular mutation. If we rescale the concentration  $c$  of CIP by  $IC_{50}$  of the corresponding  
 155 strain,  $x = c/IC_{50}$ , and the growth rate by the null-fitness  $f(0)$ , the curves collapse to a single curve  
 156  $w(x)$  that can be approximated by the Hill function  $(1 + x^4)^{-1}$  (Figure 2B). The precise shape of the  
 157 curve is not important for further analysis. However, the data collapse suggests that we can assume  
 158 that the dose-response curve of a mutant with (relative) null-fitness  $r$  and (relative) resistance  $m$  is

$$f(c) = rw(c/m), \tag{1}$$

159 i.e. it has the same shape as the wild-type curve  $w$  except for a rescaling of the fitness and con-  
 160 centration axes. Similar scaling relations have been reported previously by *Wood et al. (2014)* and  
 161 *Chevreau et al. (2015)*. A good biological understanding of the conditions underlying this feature is  
 162 presently lacking, but it seems intuitively plausible that the shape  $w(x)$  would be robust to changes  
 163 that do not qualitatively alter the basic physiology of growth and resistance.

164 Limited epistasis in  $r$  and  $m$

165 An interesting recent finding reported by *Knopp and Andersson (2018)* is that chromosomal re-  
 166 sistance mutations in *Salmonella typhimurium* mostly alter the null-fitness as well as the MIC of  
 167 various antibiotics in a non-epistatic, multiplicative manner, i.e. if a particular mutation increases  
 168 (decreases) the resistance (null-fitness) by a factor  $k_1$ , and another mutation does the same with  
 169 a factor  $k_2$ , then the mutations jointly alter these phenotypes roughly by a factor of  $k_1 k_2$  (with a

170 few exceptions). We have done a similar comparison for the data on the null-fitness and MIC for  
 171 *E. coli* strains in *Marcusson et al. (2009)*. We have analyzed a subset of 4 mutations for which the  
 172 complete data set for all combinatorial mutants is available from *Marcusson et al. (2009)*. The data  
 173 are shown in Table 1. Out of 11 multiple-mutants, only 2 show epistasis in  $r$  and 4 show epistasis  
 174 in  $m$ . Moreover, in all cases where significant epistasis occurs it is negative, i.e. the effect of the  
 175 multiple mutants is weaker than expected from the single mutation effects.

#### 176 Formulation of the model

177 The above observations suggest a model where one assumes, as an approximation, that all the  
 178  $r$  and  $m$  values of individual mutations combine multiplicatively. A genotype with  $n$  mutations  
 179  $(r_1, m_1), (r_2, m_2), \dots, (r_n, m_n)$  has a null-fitness  $r$  and a resistance value  $m$  given by

$$r = \prod_{i=1}^n r_i \quad \text{and} \quad m = \prod_{i=1}^n m_i. \quad (2)$$

180 Moreover, the dose-response curves of the genotypes are taken to be of the scaling form (1),  
 181 where the function  $w(x)$  does not depend on the genotype. As indicated before, and without any  
 182 loss of generality, we choose units such that, for the wild type,  $r = 1$  and  $m = 1$ . Therefore the  
 183 dose-response curve of the wild type is  $w(x)$  with  $w(0) = 1$ , and choosing  $IC_{50}$  as a measure of  
 184 resistance, we have  $w(1) = \frac{1}{2}$ . Henceforth, we refer to  $x$  simply as the concentration. We also recall  
 185 that the condition of adaptational tradeoff means that  $r_i < 1$  and  $m_i > 1$  for all mutations.

186 If the  $r_i$  and  $m_i$  values combine non-epistatically, and if the shape of the dose-response curve is  
 187 known, it is thus possible to construct the entire concentration-dependent landscape of size  $2^L$  from  
 188 just  $2L$  measurements (of the  $r_i$  and  $m_i$  values of the single mutants) instead of the measurement  
 189 of  $2^L$  fitness values at every concentration. In practice we do not expect a complete lack of epistasis  
 190 among all mutations of interest, and the dose-response curve is also an approximation obtained by  
 191 fitting a curve through a finite set of fitness values known only with limited accuracy. However, the  
 192 fitness rank order of genotypes, and related topographic features such as fitness peaks, are robust  
 193 to a certain amount of error in fitness values (*Crona et al., 2017*), and our model may be used to  
 194 construct these to a good approximation.

195 Lastly, we require that the dose-response curves of the wild type and a mutant intersect at most  
 196 once, which implies that the equation  $w(x) = rw\left(\frac{x}{m}\right)$  with  $r > 1$  and  $m < 1$  has at most one solution.  
 197 This then also implies that the curves of any genotype  $\sigma$  and a proper superset of it (i.e. a genotype  
 198 which contains all the mutations in  $\sigma$  and some more) intersect at most once. This property holds  
 199 for all functions that have been used to represent dose-response curves in the literature, such as  
 200 the Hill function, the half-Gaussian or the exponential function, as well as for all concave function  
 201 with negative second derivate (see Materials and Methods for details).

#### 202 **Properties of tradeoff-induced fitness landscapes**

203 To understand the evolutionary implications of our model, we first describe how the fitness land-  
 204 scape topography changes with the environmental parameter represented by the antibiotic concen-  
 205 tration. Next we analyze the properties of mutational pathways leading to highly fit genotypes.

#### 206 Intersection of curves and changing landscapes

207 We start with a simple example of  $L = 2$  mutations and a Hill-shaped dose-response curve  $w(x) =$   
 208  $\frac{1}{1+x^2}$  (Figure 3). At  $x = 0$ , the rank ordering is determined by the null-fitness. The wild type has  
 209 maximal fitness, and the double mutant is less fit than the single mutants. As  $x$  increases, the  
 210 fitness curves start to intersect, and each intersection switches the rank of two genotypes. In the  
 211 present example we find a total of six intersections and therefore seven different rank orders  
 212 across the full range of  $x$ . This is actually the maximum number of rank orders that can be found  
 213 by scanning through  $x$  for  $L = 2$ , see Materials and Methods. The final fitness rank order ( in the  
 214 region G in Figure 3A) is the reverse of the original rank order at  $x = 0$ . Figure 3B depicts the

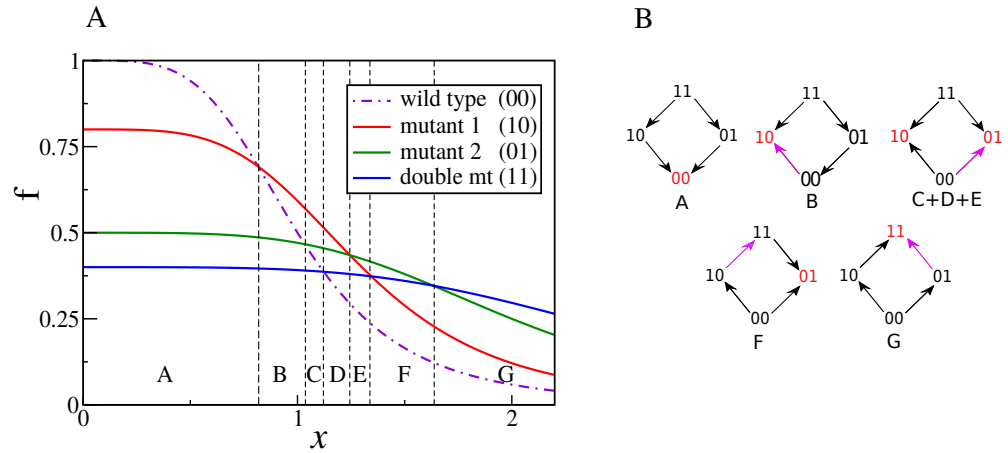


**Figure 3. (A)** An example of dose-response curves of four genotypes – the wild type (00), two single mutants (10 and 01), and the double mutant (11). The parameters of the two single mutants are  $r_1 = 0.8$ ,  $m_1 = 1.3$ ,  $r_2 = 0.5$ ,  $m_2 = 2.5$ . Null-fitness and resistance combine multiplicatively, which implies that the parameters of the double mutant are  $r_{12} = r_1 r_2 = 0.4$  and  $m_{12} = m_1 m_2 = 3.25$ . **(B)** Fitness graphs corresponding to antibiotic concentration ranges from panel **(A)**. The genotypes in red are the local fitness peaks. The purple arrows are the ones that have changed direction at the beginning of each segment. All arrows eventually switch from the downward to the upward direction.

215 concentration-dependent fitness landscape of the 2-locus system in the form of fitness graphs.  
 216 A fitness graph represents a fitness landscape as a directed graph, where neighboring nodes are  
 217 genotypes that differ by one mutation, and arrows point toward the genotypes with higher fitness  
 218 (*de Visser et al., 2009; Crona et al., 2013*). A fitness graph does not uniquely specify the rank  
 219 order in the landscape (*Crona et al., 2017*). For example, the three regions C, D and E have different  
 220 rank orders but the same fitness graph. Because selection drives an evolving population towards  
 221 higher fitness, a fitness graph can be viewed as a roadmap of possible evolutionary trajectories.  
 222 In particular, a fitness peak (marked in red in Figure 3B) is identified from the fitness graph as  
 223 a node with only incoming arrows. Fitness graphs also contain the complete information about  
 224 the occurrences of sign epistasis. Sign epistasis with respect to a certain mutation occurs when  
 225 the mutation is beneficial in some backgrounds but deleterious in others (*Weinreich et al., 2005*;  
 226 *Poelwijk et al., 2007*). It is easy to read off sign epistasis for a mutation from the fact that parallel  
 227 arrows (i.e. arrows corresponding to the gain or loss of the same mutation) in a fitness graph point  
 228 in opposite directions.

229 For example, in the graph for the region B there is sign epistasis in the first position, since the  
 230 parallel arrows  $00 \rightarrow 10$  and  $01 \leftarrow 11$  point in opposite directions. Notice that in the current example,  
 231 we start with a smooth landscape at  $x = 0$  (as seen in the fitness graph for region A), and the  
 232 number of peaks and the degree of sign epistasis both reach a maximum in the intermediate region  
 233 C+D+E. This fitness graph displays reciprocal sign epistasis, which is a necessary condition for the  
 234 existence of multiple fitness peaks (*Poelwijk et al., 2011*). Beyond the region E, the landscape starts  
 235 to become smooth again, with only one fitness maximum and a lower degree of sign epistasis. In  
 236 the last region G, the landscape is smooth with only one peak (the double mutant 11) and no sign  
 237 epistasis.

238 These qualitative properties generalize to larger landscapes. To show this, we consider a  
 239 statistical ensemble of landscapes with  $L$  mutations, where the parameters  $r_i, m_i$  of single mutations  
 240 are independently and identically distributed according to a joint probability density  $P(r, m)$ . Figure 4  
 241 shows the result of numerical simulations of these landscapes for  $L = 16$ . The mean number of  
 242 fitness peaks with  $n$  mutations reaches a maximum at  $x_{\max}(n)$  where to leading order  $\log x_{\max}(n) \sim$

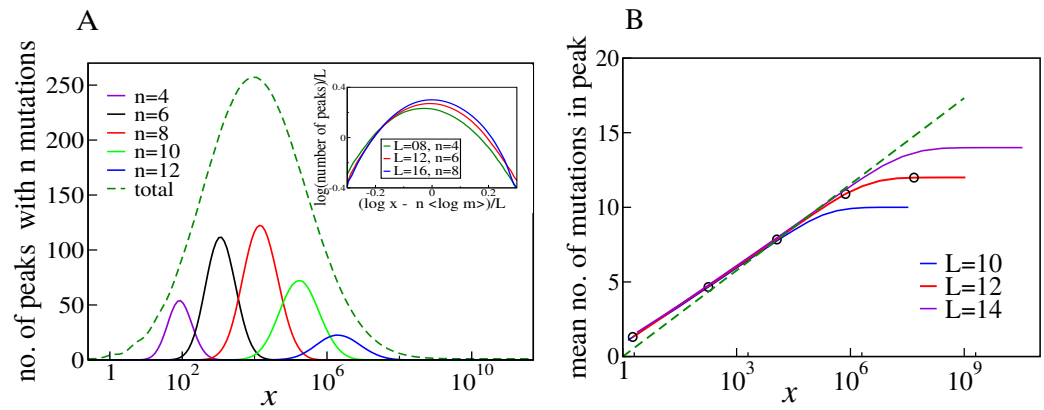


**Figure 4. (A)** Number of fitness peaks as a function of concentration for different numbers of mutations in the peak,  $n$ , and  $L = 16$ . The dashed green curve is the total number of fitness peaks, summed over  $n$ . The peaks were found by numerically generating an ensemble of landscapes with individual effects distributed according to the joint distribution (8). For this distribution,  $\langle \log m \rangle = 1.19645$ . Inset: The maximal number of peaks for a given value of  $n$  occurs at  $\log x_{\max}(n) = n \langle \log m \rangle$ , and grows exponentially with  $L$ . **(B)** Mean number of mutations in a fitness peak as a function of concentration  $x$  for the same model. The black circles are the mean number of mutations in the fittest genotype. The green dashed line is  $\frac{\log(x)}{\langle \log m \rangle}$ , where  $\langle \log m \rangle = 1.19645$  as before.

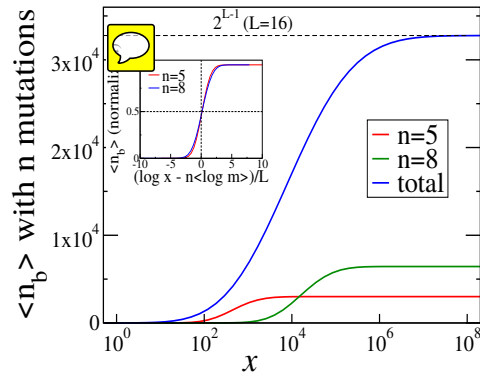
243  $n \langle \log m \rangle$ , independent of any further details of the system, as argued in Materials and Methods.  
 244 The asymptotic expression works well already for  $L = 16$  (see inset of Figure 4A). Figure 4B shows  
 245 the mean number of mutations in a fitness peak. This is well approximated by the curve  $n =$   
 246  $\frac{\log x}{\langle \log m \rangle}$ , showing that the mean number of mutations in a fitness peak grows logarithmically in the  
 247 concentration. This is consistent with what we would expect from the variation in the number of  
 248 peaks with  $n$  mutations as shown in Figure 4A. The existence of a typical number of mutations in a  
 249 fitness peak is one of the distinctive features of our landscape, a feature typically lacking in other  
 250 well-studied random landscape models. This property arises from the existence of adaptational  
 251 tradeoffs. Since a high number of mutations is beneficial at higher concentrations but deleterious  
 252 at lower concentrations, it is clear that there must be an optimal number of mutations at some  
 253 intermediate concentration.

254 As another indicator of ruggedness, we consider the number of backgrounds in which a mutation  
 255 is beneficial as a function of  $x$ . At  $x = 0$ , any mutation is deleterious in all backgrounds, whereas at  
 256 very large  $x$  it is beneficial in all backgrounds. Therefore there is no sign epistasis in either case.  
 257 Sign epistasis is maximized when a mutation is beneficial in exactly 1/2 of all backgrounds. Figure 5  
 258 shows the mean number of backgrounds  $n_b$  (with  $n$  mutations each) in which the occurrence a  
 259 mutation is beneficial, for two different values of  $n$ . The curves have a sigmoidal shape, starting from  
 260 zero and saturating at  $\binom{L}{n}$ , which is the total number of backgrounds with  $n$  mutations. The blue  
 261 curve shows the mean total number of backgrounds (with any  $n$ ) in which a mutation is beneficial,  
 262 which has a similar shape. Since every mutation in every background goes from being initially  
 263 deleterious to eventually beneficial, there must be some  $x$  at which every mutation is beneficial in  
 264 exactly half the backgrounds. The inset of Figure 5 shows that for backgrounds with  $n$  mutations,  
 265 the average concentration at which a mutation is beneficial in 1/2 the backgrounds is given by  
 266  $\log x \simeq n \langle \log m \rangle$ , which is the same concentration at which the largest number of fitness peaks were  
 267 found in Figure 4. A derivation of this relation is given in Materials and Methods. Similarly, when  
 268 summed over all mutation numbers  $n$ , the fraction of beneficial backgrounds reaches 1/2 around  
 269 the same concentration at which the total number of fitness peaks is maximal. Since the number of  
 270 backgrounds is largest at  $n = L/2$  for combinatorial reasons, this concentration is approximately  
 271 given by  $\log x \simeq \frac{L}{2} \langle \log m \rangle$ .

272 **Complementary to these results about the background dependence of the sign of mutational**



273 effects, it can be shown that any two distinct sets of mutations occurring in any genetic background  
 274 show sign epistasis at some value of  $x$ . This  
 275 is a consequence of the rank ordering properties of the landscapes that are described in  
 276 the next subsection (see Materials and Methods for a proof). A special case is that any  
 277 two single mutations occurring in the wild type  
 278 background must exhibit pairwise sign epis-  
 279 tasis at some concentration.



286 **Figure 5.** The mean number of genetic backgrounds  $n_b$   
 287 in which a mutation is beneficial depends on the  
 288 concentration. The numerically computed mean  
 289 number is shown in the blue curve. We also computed  
 290 the mean  $n_b$  for genetic backgrounds with a fixed a  
 291 number  $n$  of mutations. The results for two of these  
 292 values,  $n = 5$  and  $n = 8$  are also shown. The inset shows  
 293 these values of mean  $n_b$  as a fraction of the total  
 294 number of backgrounds with  $n$  mutations.

295  
 296  
 297  
 298 path exists from the initial to the final genotype.

299 The accessibility of peaks in a fitness landscape is determined by the rank ordering of the geno-  
 300 types. We now show that the rank orders of tradeoff-induced fitness landscapes are constrained in  
 301 a way that gives rise to unusually high accessibility. Consider two distinct sets of **one or more** muta-  
 302 tions  $A_i$  and  $A_j$  that can occur on the genetic background  $W$ , and the four genotypes  $W$ ,  $WA_i$ ,  $WA_j$   
 303 and  $WA_iA_j$ , where a concatenation of symbols represents the genotype which contains all the  
 304 mutations referred to by the symbols. The **ordering condition** (derived in Materials and Methods)  
 305 says that whenever  $W$  is the fittest among these four genotypes,  $WA_iA_j$  must be the least fit, and  
 306 whenever  $WA_iA_j$  is the fittest,  $W$  must be the least fit. For the case of two single mutations this  
 307 situation is illustrated by the fitness graphs in Figure 3B, where the background genotype  $W = 00$   
 308 is the fittest in the first segment A and the genotype  $WA_iA_j = 11$  is the fittest in the last segment  
 309 G. The ordering condition has the immediate consequence that **at all environments  $x$** , the fittest  
 310 genotype is *always* accessible from the background genotype  $W$ . If the fittest genotype is one  
 311 of the **single mutants** (segments B, C, D and F), then it is of course accessible. If it is the **double**  
 312 **mutant**  $WA_iA_j$  (segment G), then the background genotype must be the least fit genotype (from the  
 313 ordering condition), and therefore  $WA_i$  and  $WA_j$  should be fitter than  $W$ . Then  $WA_iA_j$  is accessible  
 314 from the wild type through the path  $W \rightarrow WA_i \rightarrow WA_iA_j$  and the path  $W \rightarrow WA_j \rightarrow WA_iA_j$ .

315 To fully exploit the consequences of the ordering property we need to introduce some notation.  
 316 Let  $\sigma$  be a genotype with  $n$  mutations. We define a *subset* of  $\sigma$  as a genotype with  $l$  mutations,  $l \leq n$ ,  
 317 which are all contained in  $\sigma$  as well. Likewise, a *superset* of  $\sigma$  is a genotype with  $l$  mutations,  $l \geq n$ ,  
 318 that contains all the mutations in  $\sigma$ . With this, the ordering condition can be seen to imply that  
 319 the superset of a fitness peak is accessible from its own supersets. For example, if  $W$  is the fittest  
 320 genotype, then  $WA_i$  is a superset of it, and because of the ordering condition,  $WA_i$  must be fitter  
 321 than its superset  $WA_iA_j$ , and therefore accessible from it. Similarly, it is easy to show that the  
 322 subset of a fitness peak is accessible from its own subsets. This property can be generalized and

### Accessibility of fitness peaks

Having shown that tradeoff-induced fitness landscapes display a large number of fitness peaks at intermediate concentrations, we now ask how these peaks affect the evolutionary dynamics. We base the discussion on the concept of evolutionary accessibility, which effectively assumes a regime of weak mutation and strong selection (Gillespie, 1984). In this regime the evolutionary trajectory consists of a series of fixation events of beneficial single-step mutations represented by a directed path in the fitness graph of the landscape (Weinreich et al., 2005, 2006; Franke et al., 2011). We say that a genotype is *accessible* from another genotype if a directed

323 constitutes our main result on accessibility of fitness peaks.

324 **Accessibility property:** Any genotype  $\Sigma$  that is a superset of a local fitness peak  $\sigma$  is accessible from  
 325 all the superset genotypes of  $\Sigma$ . Similarly, any genotype  $\Sigma'$  that is a subset of a local fitness peak  $\sigma$  is  
 326 accessible from all the subset genotypes of  $\Sigma'$ .

327 The proof is given in Materials and Methods. Three particularly important consequences are

- 328 • Any fitness peak is accessible from all its subset and superset genotypes.
- 329 • **Any fitness peak is accessible from the wild type.** This is because the wild type is a subset  
 330 of every genotype.
- 331 • For the same reason, when the wild type is a fitness peak (e.g., at  $x = 0$ ), it is accessible from  
 332 every genotype, and is therefore also the only fitness peak in the landscape. The same holds  
 333 for the all-mutant when  $x$  is sufficiently large, since it is a superset of every genotype.

334 These properties are illustrated by the fitness graph in Figure 6. We assume in some environment  $x$   
 335 that the landscape has (at least) two peaks at the genotypes 1001 (marked in red) and 0111 (marked  
 336 in blue). The colored arrows point towards mutational neighbors with higher fitness and are  
 337 enforced by the accessibility property. The edges without arrowheads are not constrained by the  
 338 accessibility property and the corresponding arrows (which are not shown in the figure) could point  
 339 in either direction. Consider the genotype 0111 (marked in blue). It is accessible from all its subsets,  
 340 namely 0000, 0010, 0010, 0001, 0110, 0101 and 0011, following the upward pointing blue arrows. These  
 341 subsets are in turn accessible from their subsets. For example, 0011 is accessible from all its subsets  
 342 – 0000, 0010, and 0001. The fitness peak is also accessible from its superset 1111. The same property  
 343 holds for the other fitness peak. The subsets or supersets may access the fitness peaks using other  
 344 (unmarked) paths as well, which would include one or more of the undirected lines in conjunction  
 345 with some of the arrows. Moreover, other genotypes, which are neither supersets nor subsets, may  
 346 also access these fitness peaks through paths that incorporate some of the undirected edges.

347  
 348  
 349  
 350  
 351  
 352  
 353  
 354  
 355  
 356  
 357  
 358  
 359  
 360  
 361  
 362  
 363  
 364  
 365  
 366  
 367  
 368  
 369  
 370  
 371  
 372

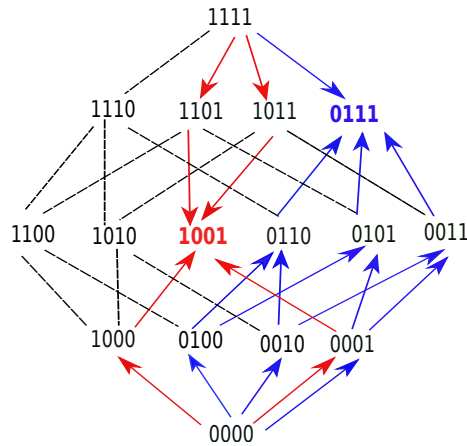


**Figure 6.** A fitness graph of a landscape with  $L = 4$  mutations, illustrating the accessibility property. There are two fitness peaks, 1001 (red) and 0111 (blue). The fitness peaks are accessible from all their subset and superset genotypes following the paths marked by the arrows.

A fitness peak together with its subset and superset genotypes defines a sub-landscape with remarkable properties. It is a smooth landscape with only one peak which is accessible from any genotype via all direct paths, i.e. paths where the number of mutations monotonically increases or decreases. For example, the fitness peak 1001 is accessible from the all-mutant 1111 by the two direct paths – 1111 → 1101 → 1001 and 1111 → 1011 → 1001. Likewise, the peak 0111 is accessible from its subset 0001 via the paths 0001 → 0101 → 0111 and 0001 → 0011 → 0111. In general, a peak with  $n$  mutations is accessible from a subset genotype with  $m$  mutations by  $(n - m)!$  direct paths, and from a superset genotype with  $m$  mutations by  $(m - n)!$  direct paths. This gives a lower bound on the total number of paths by which a fitness peak is accessible from a subset or superset genotype.

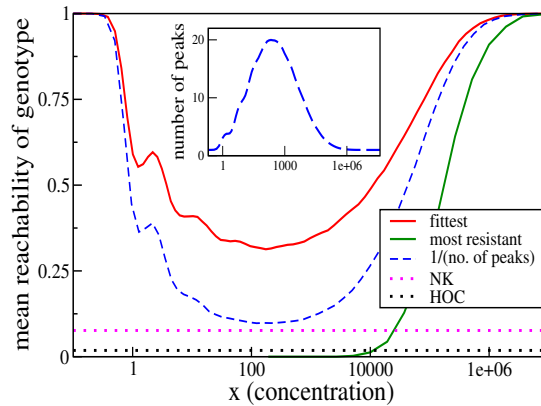
Importantly, the accessibility property formulated above holds under more general conditions than stipulated in the model. We show in Materials and Methods that it holds whenever the null fitness and resistance values of the mutations,  $r$  and  $m$ , do not show *positive* epistasis. This is a weaker requirement than our original assumption of a strict lack of epistasis in these two phenotypes.

373 In this context it should be noted that the rank orderings forbidden by the ordering condition all  
 374 show positive epistasis for the fitness values, whereas all the allowed orderings can be constructed  
 375 without positive epistasis. Therefore, any landscape where positive epistasis in fitness is absent will  
 376 also display the accessibility property. However, whereas the lack of positive epistasis is a sufficient  
 377 condition, it is not necessary. In particular, our model does allow for cases of positive epistasis in  
 378 the fitness values.

### 379 Reachability of the fittest and the most resistant genotype


380 The preceding analyses have shown that within the mutant selection window, where mutants with  
 381 higher fitness than the wild type exist, every fitness peak is accessible from the wild type. This  
 382 includes in particular the fittest genotype at a given concentration. However, in general there will  
 383 be many peaks in the fitness landscape, and it is not guaranteed that evolution will reach the fittest  
 384 genotype. One can ask for the probability that the fittest genotype is actually accessed under the  
 385 evolutionary dynamics, which we call its reachability. We assume that the dynamics is in the strong  
 386 selection weak mutation (SSWM) regime, and the population is large enough such that the fixation  
 387 probability of a mutant with selection coefficient  $s$  is  $1 - e^{-2s}$  for  $s > 0$ , and 0 for  $s \leq 0$  (Gillespie,  
 388 1984). In our setting the selection coefficient is  $s = \frac{f_1}{f_0} - 1$ , where  $f_1$  is the growth rate of a mutant  
 389 appearing in a population of cells with growth rate  $f_0$ .

390 Figure 7 shows the numerically obtained reachability for  $L = 10$ , averaged over the distribution  
 391  $P(r, m)$  given in Eq. (8). The reachability of the highest peak is 1 at very low and very high concentra-  
 392 tions, since there is only peak, the wild type or the all-mutant, at these extremes. The reachability is  
 393 lower at intermediate concentrations, where there are multiple peaks, all of which are accessible  
 394 from the wild type. The dashed blue line is the mean of the reciprocal of the total number of fitness  
 395 peaks, and is therefore the mean reachability of fitness peaks. The reachability of the highest  
 396 peak follows the qualitative behavior of the mean reachability, but remains higher than the mean  
 397 reachability everywhere.



411 **Figure 7.** Reachability of fittest genotype and most  
 412 resistant genotype. The same model as in the previous  
 413 subsection has been used, with  $L = 10$ . Inset shows the  
 414 mean number of fitness peaks as a function of  
 415 concentration. Dotted horizontal lines show  
 416 comparisons to the HoC model and an NK model with  
 417 the same number of mutations. These models were  
 418 implemented using an exponential distribution of  
 fitness values.

420  
 421 We would therefore naturally expect a smaller fraction of adaptive walks to  
 422 terminate at the fittest peak. A more illuminating comparison is with the NK model (Kauffman and

The green curve is the reachability of the most resistant genotype, i.e the all-mutant. It is extremely low at low and moderate concentrations and grows steeply and saturates quickly at a very large concentration. The all-mutant genotype is less-than-average reachable everywhere except at very high concentration, when it is the only fitness peak and accessible from every other genotype. 

We have compared the reachability to two other widely studied landscape models. One is the House-of-Cards (HoC) model (Kauffman and Levin, 1987; Kingman, 1978), where each genotype is independently assigned a fitness value drawn from a continuous distribution. The reachability is found to be around 0.018, an order of magnitude smaller than the lowest reachability seen in the tradeoff-induced landscape. The mean number of fitness maxima in the HoC landscape is  $\frac{2^L}{L+1}$ , which in this case is approximately 93.1, much higher than the maximum mean number of peaks in the tradeoff-induced landscape (in-

423 *Weinberger, 1989; Hwang et al., 2018*). Here, once again,  $L = 10$ , and the mutations are divided  
 424 into two blocks of 5 mutations each. As per the usual definition of the model, the fitness of a  
 425 genotype is the sum over the contributions of each of the 10 mutations, and the contribution of  
 426 each mutation depends only the state of the block to which it belongs. The fitness contribution of  
 427 each mutation for any state of the block is an independent random number. The mean number  
 428 of fitness maxima here is  $\approx 28.44$  (*Perelson and Macken, 1995; Schmiegelt and Krug, 2014*), which  
 429 is comparable to the maximum mean number in the tradeoff-induced landscapes (see inset of  
 430 Figure 7). Nonetheless, the reachability of the fittest peak (dotted pink line) is found to be nearly 4  
 431 times smaller than the lowest reachability in our landscape. We found that in a fraction of about  
 432 0.64 of the landscapes, the fittest maximum is not reached in any of 32000 dynamical runs, indicating  
 433 the absence of an accessible path in most of these cases (*Schmiegelt and Krug, 2014; Hwang et al.,*  
 434 *2018*). In contrast, an evolutionary path always exists to any fitness peak in the tradeoff-induced  
 435 landscapes, as we saw in the previous subsection. This endows the tradeoff-induced landscapes  
 436 with the unusual property of being highly rugged and at the same time having a much higher  
 437 evolutionary reachability of the global fitness maximum compared to other models with similar  
 438 ruggedness.

## 439 Discussion

440 Fitness landscapes depend on the environment, and gene-gene-interactions can be modified  
 441 by the environment. Systematic studies of such  $G \times G \times E$  interactions are rare, but they are  
 442 clearly of relevance to scenarios such as the evolution of antibiotic resistance, where the antibiotic  
 443 concentration can vary substantially in space and time. In this paper we have explored the structure  
 444 of such landscapes in the presence of tradeoffs between fitness and resistance. We summarize the  
 445 main findings of our work.

- 446 • We have shown experimental evidence that the dose-response curves of various mutant  
 447 strains of *E. coli* to the antibiotic ciprofloxacin have the same shape, except for a rescaling  
 448 of the fitness and concentration values. If this shape is known, the fitness of a strain can be  
 449 estimated at any antibiotic concentration simply by measuring its null-fitness and  $IC_{50}$  (or MIC).  
 450 This makes it possible to construct empirical fitness landscapes at any antibiotic concentration  
 451 from a limited set of data.
- 452 • Under the assumptions of our model the degree of epistasis, particularly sign epistasis, is  
 453 low for zero and high antibiotic concentrations, but it is nevertheless high in the intermediate  
 454 concentration regime. The number of local fitness peaks scales exponentially in the number  
 455 of mutations at these concentrations. Epistasis is often discussed as a property intrinsic  
 456 to mutations and their genetic backgrounds, with limited consideration of environmental  
 457 parameters. But in the landscapes studied here, the environmental parameter is of paramount  
 458 importance, since changes in it can dramatically alter gene-gene interactions.
- 459 • The expected number of mutations in a fitness peak increases logarithmically with the anti-  
 460 biotic concentration. This implies that, at a given concentration, the highly fit genotypes that  
 461 make up the fitness peaks carry an optimal number of mutations that arises from the tradeoff  
 462 between fitness cost and resistance.
- 463 • Despite the high ruggedness, the landscape displays strong non-random patterns. A rank  
 464 ordering condition between sets of mutations holds at all concentrations. A remarkable and  
 465 unexpected consequence of this is that any fitness peak is evolutionarily accessible from the  
 466 wild type.
- 467 • It is well known from experimental studies of antimicrobial resistance evolution that highly  
 468 resistant genotypes often require multiple mutations which can be acquired along different  
 469 evolutionary trajectories. Epistatic interactions constrain these trajectories and are generally  
 470 expected to impede the evolution of high resistance. We find that strong and complex epistatic  
 471 interactions inevitably arise in the mutant selection window, but at the same time the evolution

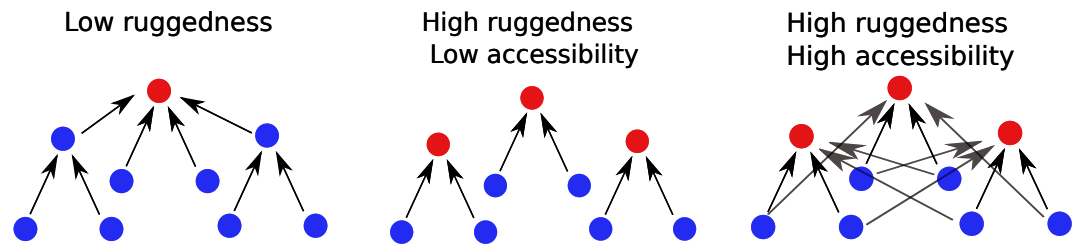


**Figure 8. Accessibility and ruggedness in different types of fitness landscapes:** The first two landscapes correspond to the typical cases of smooth and rugged landscapes. The third figure describes landscapes with adaptational tradeoffs, where high ruggedness coexists with high accessibility.

472 of the most resistant genotype (the identity of which changes with concentration) remains  
473 facile and can occur along many different pathways.

474 All of these conclusions follow from three basic assumptions that are readily generalizable  
475 beyond the context of antimicrobial resistance evolution: the existence of tradeoffs between two  
476 *marginal phenotypes* that govern the adaptation at extreme values of an environmental parameter;  
477 the scaling property of the shape of the tradeoff function; and the condition of limited epistasis  
478 for the marginal phenotypes. How generally these assumptions are valid is a matter of empirical  
479 investigation. We have shown that they hold for certain cases, and the interesting evolutionary  
480 implications of our results indicate that more empirical research in this direction will be useful.

481 In the case of antimicrobial resistance, there can be fitness compensatory mutations (*Levin*  
482 *et al., 2000; Brown et al., 2010; Durão et al., 2018*) that do not exhibit any adaptational tradeoffs.  
483 These mutations are generally found in a population in the later stages of the evolution of antibiotic  
484 resistance, which implies that they emerge in a genetic background of mutations with adaptational  
485 tradeoffs. An understanding of tradeoff-induced landscapes is therefore a prerequisite for predict-  
486 ing the emergence of compensatory mutations. [While compensatory mutations are expected to](#)  
487 [facilitate the evolution of high resistance \(Hughes and Andersson, 2017\), our study shows that the](#)  
488 [acquisition of multiple resistance mutations may readily occur even if compensatory mutations are](#)  
489 [absent.](#)

490 In the formulation of our model we have assumed for convenience that the marginal phenotypes  
491 combine multiplicatively, but this assumption is in fact not necessary for all our results. As shown  
492 in Materials and Methods, our key results on accessibility only require the absence of positive  
493 epistasis. These results therefore hold without exception for the combinatorially complete data set  
494 in Table 1, where epistasis is either absent or negative. More generally, our analysis remains valid in  
495 the presence of the commonly observed pattern of diminishing returns epistasis among beneficial  
496 mutations (*Chou et al., 2011; Schoustra et al., 2016; Wünsche et al., 2017*). We expect our results  
497 to hold approximately even when there is a small degree of epistasis (positive or negative) in  $r$  and  
498  $m$ , but we do not explore that question quantitatively in this paper.

499 [A strict absence of epistasis, while certainly not universal, can be expected to occur under](#)  
500 [certain generic circumstances. Assuming that we deal with a single antibiotic that has a single](#)  
501 [target enzyme, we can think of two situations that could lead to a multiplicative behaviour of  \$IC\_{50}\$ .](#)  
502 [\(i\) Single mutations occur in different genes that affect the concentration of the antibiotic-target](#)  
503 [enzyme complex through independent mechanisms. \(ii\) Single mutations occur in the same gene](#)  
504 [but their effect is multiplicative due to the nature of antibiotic-enzyme molecular interactions.](#)  
505 [An example of scenario \(i\) would be a combination of mutations in the target gene \(reduction of](#)  
506 [the binding affinity\), its promoter \(increase in expression\), genes regulating the activity of efflux](#)  
507 [pumps and porins \(decrease in intracellular concentration of the antibiotic\), or genes controlling](#)  
508 [the level \(increase in concentration\) or activity of drug-degrading enzymes. These mechanisms are](#)  
509 ["orthogonal" to each other, in the sense that they modify independent pathways within the cell. If](#)  
510 [each of them affects the concentration of the antibiotic-target complex through first-order kinetics,](#)

511 their cumulative effect will be multiplicative in terms of the  $IC_{50}$ s of single mutations.

512 In the case of ciprofloxacin and *E. coli* (Figure 2 and Table 1), we expect mutations in *gyrA* (target)  
 513 to be orthogonal mutations in *acrR* and *marR* (efflux pumps). This is borne out by the observed  
 514 multiplicativity of  $IC_{50}$  (Table 1). As for scenario (ii), the single mutations must affect different parts  
 515 of the antibiotic-enzyme binding site independently. This is not the case for two different mutations  
 516 in *gyrA* – S83L and D87N (see cases of epistasis in Table 1). An example for scenario (ii) are the  
 517 two mutations P21L and A26T in the gene encoding the enzyme dihydrofolate reductase, which  
 518 increase the resistance to trimethoprim in a multiplicative way in the absence of other mutations  
 519 (Palmer *et al.*, 2015). If the antibiotic has more than one target, multiplicativity would not generally  
 520 hold. In particular, topoisomerase IV (gene *parC*) is a secondary target for ciprofloxacin with much  
 521 weaker affinity than gyrase. Therefore, mutations in *parC* do not contribute to resistance unless  
 522 there is already a mutation in *gyrA*.

523 The co-existence of high ruggedness and high accessibility found in the tradeoff-induced land-  
 524 scapes studied here is counterintuitive, and to the best of our knowledge fitness landscape models  
 525 with this property have not been described previously. The situation is depicted schematically in  
 526 Figure 8. The first landscape is smooth with a single peak that must be accessible from everywhere  
 527 else. The second landscape is rugged, and each fitness peak is typically accessible from a few  
 528 genotypes only. This is the typical picture of a rugged fitness landscape with limited accessibility, as  
 529 it would be predicted by simple statistical models such as the HoC, NK or rough Mt. Fuji models  
 530 (Szendro *et al.*, 2013; Neidhart *et al.*, 2014; Hwang *et al.*, 2018). The landscapes we describe here  
 531 belong to a third type, where a high number of peaks are accessible from a high number of geno-  
 532 types, creating overlapping “valleys” from which a population may evolve towards different local  
 533 fitness maxima. Moreover, not only are fitness peaks accessible from all their subset and superset  
 534 genotypes, but there are many direct paths leading up to each peak. This appears contrary to  
 535 the expectation that in landscapes with high epistasis, accessibility should be facilitated through  
 536 mutational reversions, i.e indirect paths (DePristo *et al.*, 2007; Palmer *et al.*, 2015; Wu *et al.*, 2016;  
 537 Zagorski *et al.*, 2016).

538 We conclude with some possible directions for future work. Our model provides a principled  
 539 framework for predicting how microbial fitness landscapes vary across different antibiotic concen-  
 540 trations. This could be exploited to describe situations where the antibiotic concentration varies  
 541 on a time scale comparable to the evolution of resistance, either due to the degradation of the  
 542 drug or by an externally imposed treatment protocol (Marrec and Bitbol, 2018). In this context it  
 543 would be of particular interest to include compensatory mutations that lack the tradeoff between  
 544 growth and resistance, since such mutations are expected to strongly affect the extent to which  
 545 resistance can be reversed (Andersson and Hughes, 2010). Significant extension of the theory is  
 546 required if the drug concentration varies on a faster time scale comparable to the growth time of  
 547 the microbial population, in which case the concept of a concentration-dependent fitness would  
 548 need to be reconsidered.

549 From the broader perspective of evolutionary systems with adaptational tradeoffs mediated by  
 550 an environmental parameter, our study makes the important conceptual point that it is impossible  
 551 to have non-epistatic fitness landscapes for all environments. Using the terminology of Gorter *et al.*  
 552 (2016), the tradeoffs enforce reranking  $G \times E$  interactions which in turn, as we have shown, induce  
 553 sign-epistatic  $G \times G$  interactions at intermediate values of the environmental parameter. Notably,  
 554 this general conclusion does not depend on the scaling property of the tradeoff function. It would  
 555 nevertheless be of great interest to identify instances of scaling for other types of adaptational  
 556 tradeoffs, in which case the detailed predictions of our model could be applied as well.

## 557 Acknowledgements

558 We thank Douglas Huseby and Diarmaid Hughes for providing us with the *E. coli* strains of Marcusson  
 559 *et al.* (2009), and Tobias Bollenbach, Michael Brockhurst and Kristina Crona for useful comments.  
 560 The work of SGD and JK was supported by DFG within CRC 1310 *Predictability in Evolution*, and

561 JK acknowledges the kind hospitality of the Scottish Universities Physics Alliance and the Higgs  
 562 Center for Theoretical Physics during the completion of the project. SOLD and RJA acknowledged the  
 563 support of the ERC Consolidator Grant 682237 EVOSTRUC.

## 564 **Materials and Methods**

### 565 **Experiments**

#### 566 **Bacterial strains**

567 We used strains from Marcusson et al. (2009) (courtesy of Douglas Huseby and Diarmaid Hughes).  
 568 The strains are isogenic derivatives of MG1655, a K12 strain of the bacterium *E. coli*, with specific  
 569 point mutations or gene deletions in five different loci: *gyrA:S83L*, *gyrA:D87N*, *parC:S80I*,  $\Delta$ *marR*, and  
 570  $\Delta$ *acrR*. There are 32 possible combinations of these alleles, but we only used the wild type, single  
 571 mutants (5 strains) and double mutants (8 strains of 10 possible combinations): LM179 (00000),  
 572 LM378 (10000), LM534 (01000), LM792 (00100), LM202 (00010), LM351 (00001), LM625 (11000),  
 573 LM862 (10100), LM421 (10010), LM647 (10001), LM1124 (01100), LM538 (01010), LM592 (01001),  
 574 LM367 (00011). A binary sequence after the strain's name represents the presence/absence of a  
 575 particular mutated allele (order as in the above list of genetic alterations).

#### 576 **Growth media and antibiotics**

577 LB growth medium was prepared according to Miller's formulation (10g tryptone, 5g yeast extract,  
 578 10g NaCl per litre). The pH was adjusted to 7.2 with NaOH, and autoclaved at 121°C for 20 min.  
 579 Ciprofloxacin (CIP) solutions were prepared from a frozen stock (10mg/ml ciprofloxacin hydrochloride,  
 580 pharmaceutical grade, AppliChem, Darmstadt, in sterile, ultra-pure water) by diluting into LB  
 581 to achieve the desired concentrations.

#### 582 **Dose-response curves**

583 We incubated bacteria in 96-well clear flat bottom micro-plates (Corning Costar) inside a plate reader  
 584 (BMG LABTECH FLUOstar Optima with a stacker) starting from two different initial cell densities (half  
 585 a plate for each), and measured the optical density (OD) of each culture every 2-5 min to obtain  
 586 growth curves. Plates were prepared automatically using a BMG LABTECH CLARIOstar plate reader  
 587 equipped with two injectors connected to a bottle containing LB and a bottle with a solution of CIP  
 588 in LB. The injectors were programmed to create different concentrations of CIP in each column of  
 589 the 96 well plate. The injected volumes of the CIP solution were 0, 20, 25, 31, 39, 49, 62, 78, 98,  
 590 124, 155, 195  $\mu$ l, and an appropriate volume of LB was added to bring the total volume to 195  $\mu$ l  
 591 per well. Since different strains had MICs spanning almost two decades of CIP concentrations, we  
 592 used a different maximum concentration of the CIP solution for each strain (approximately 1.5 - 2  
 593 times the expected MIC). Bacteria were diluted from a thawed frozen stock  $10^3$  and  $10^4$  times in PBS  
 594 (phosphate buffered saline buffer), and 5  $\mu$ l of the suspension was added to each well ( $10^3$  dilution  
 595 to rows A-D,  $10^4$  dilution to rows E-H). We used one strain per plate and up to 4 plates per strain  
 596 (typically 1-2). After adding the suspension of bacteria to each well, the plates were immediately  
 597 sealed with a transparent film to prevent evaporation, and put into a stacker (37°C, no shaking),  
 598 from which they would be periodically fed into the FLUOstar Optima plate reader (37°C, orbital  
 599 shaking at 200rpm for 10s prior to OD measurement). We then used the time shift methods to  
 600 obtain exponential growth rates for each strain and different concentrations of CIP, see *Ojtic et al.*  
 601 (2019) for further details.

### 602 **Mathematical Methods**

#### 603 **Rank orders and fitness graphs**

604 The total number of possible rank orders with  $L$  mutations is  $2^L!$ , which is 24 for  $L = 2$ . Not all these  
 605 rank orders, however, can be realized as one scans through  $x$ . Since any two curves intersect at  
 606 most once, the maximum number of distinct rank orders that can be reached is the rank order at

607  $x = 0$  plus the total number of possible intersections, which is  $\binom{2^L}{2} = 2^{L-1}(2^L - 1)$ . Thus the upper  
 608 bound on the number of rank orders found by scanning through  $x$  is  $2^{L-1}(2^L - 1) + 1$ , which is smaller  
 609 than  $2^L!$  for  $L \geq 2$ .

610 It is also instructive to determine the number of fitness graphs that can be found by varying  $x$  for  
 611 a system with  $L$  mutations. This can be computed as follows: At  $x = 0$  every mutation is deleterious,  
 612 and every mutational neighbor with one less mutation is fitter; but due to the tradeoff condition, at  
 613 sufficiently large  $x$  every mutation is beneficial and any mutational neighbor with one less mutation  
 614 is less fit. In order for this reversal of fitness order to happen, the dose-response curves of any two  
 615 mutational neighbors must intersect at some  $x$ . Therefore, the number of fitness graphs generated  
 616 is equal to the number of distinct pairs of mutational neighbors, which is  $2^{L-1}L$ , and the number of  
 617 distinct fitness graphs encountered is  $2^{L-1}L + 1$ . For  $L = 2$ , this number is 5, as seen in the example  
 618 in the main text.

619 **Condition for two dose-response curves to intersect at most once**

620 Consider two DR curves characterized by  $(r, m)$  and  $(r', m')$ , where  $r < r'$  and  $m > m'$ . We need to  
 621 show that for the commonly observed cases, the curves  $rw(\frac{x}{m})$  and  $r'w(\frac{x}{m'})$  intersect at most once.  
 622 First, notice that it is sufficient to prove this for the case  $r' = 1, m' = 1$ , because any rescaling of the  
 623  $x$  and  $w$  axes does not alter the number or ordering of intersection points. Therefore we require  
 624  $r < 1$  and  $m > 1$ .

625 Let us consider the case where the dose-response curve is of the form of a Hill function, i.e  
 626  $w(x) = \frac{1}{1+x^a}$ , with  $a > 0$ . The intersection of curves happens at the solution of  $w(x) = rw(\frac{x}{m})$ , which  
 627 we denote by  $x^*(r, m)$ . In this case the solution is given by

$$x^*(r, m) = \left( \frac{1-r}{r - \frac{1}{m^a}} \right)^{\frac{1}{a}}$$

628 which is positive and unique if  $rm^a > 1$ ; otherwise no solution with  $x^* > 0$  exists. It is similarly easy  
 629 to show that at most one intersection point exists for exponentials, stretched exponentials, and  
 630 half-Gaussians.

631 The property also holds for any concave dose-response curve with  $w''(x) < 0$ . We prove this as  
 632 follows. Any intersection point  $x^*$  is the solution of

$$F(x^*) = r$$

633 where  $F(x) \equiv \frac{w(x)}{w(\frac{x}{m})}$ . We will show that  $F(x)$  is monotonic and therefore the above equation has at  
 634 most one solution. We have

$$F'(x) = \frac{w'(x)w(\frac{x}{m}) - \frac{1}{m}w(x)w'(\frac{x}{m})}{w(\frac{x}{m})^2},$$

635 and  $F'(x)$  has the same sign as the numerator  $\mathcal{N}(x) = w'(x)w(\frac{x}{m}) - \frac{1}{m}w(x)w'(\frac{x}{m})$ . Since  $w(x)$  is a  
 636 decreasing function and  $m > 1$ ,  $w(\frac{x}{m}) > w(x) > \frac{1}{m}w(x)$ . When  $w''(x) < 0$ , we also have  $w'(x) < w'(\frac{x}{m})$ .  
 637 Since  $w'(x) < 0$ , this implies  $|w'(x)| > |w'(\frac{x}{m})|$ , and  $\mathcal{N}(x) < 0$ . Therefore  $F(x)$  is monotonically  
 638 decreasing.

639 **Proof of the accessibility property**

640 To derive the ordering condition, let us start with the simplest case of two single mutations  $A_i, A_j$   
 641 occurring on the wild type background. There are correspondingly four different genotypes  $W, A_i,$   
 642  $W A_i, W A_j, W A_i A_j$ , which are listed in decreasing order of fitness at  $x = 0$ . Let the intersection of  
 643 the DR curves of two genotypes  $\sigma_1$  and  $\sigma_2$  occur at  $x = X_{\sigma_1, \sigma_2}$ . Then  $X_{W, W A_j}$  is given by the solution  
 644  $x^*(r_j, m_j)$  of

$$w(x) = r_j w\left(\frac{x}{m_j}\right),$$



645 and  $X_{W A_i, W A_i A_j}$  is given by the solution of

$$r_i w\left(\frac{x}{m_i}\right) = r_i r_j w\left(\frac{x}{m_i m_j}\right).$$

646 This last equation can be re-written as

$$w(x') = r_j w\left(\frac{x'}{m_j}\right),$$

647 where  $x' = \frac{x}{m_i}$ . Comparing this with the first equation above, we have

$$X_{W A_i, W A_i A_j} = m_i X_{W, W A_j} > X_{W, W A_j}. \quad (3)$$

648 This equation tells us that whenever the double mutant is fitter than one of the single mutants, the  
 649 wild type must be less fit than the *other* single mutant. Consequently, when the double mutant is  
 650 fitter than both the single mutants, the WT must be less fit than both the single mutants. In other  
 651 words, the number of single mutants fitter than the wild type cannot be less than the number of  
 652 single mutants less fit than the double mutant. This is the ordering condition given in the main text.  
 653 Any ordering that violates this condition is a *forbidden ordering*. For greater clarity, we list all the  
 654 possible forbidden orderings (up to interchange of indices  $i$  and  $j$ ).

$$\begin{aligned} W &> W A_i > W A_i A_j > W A_j \\ W &> W A_i A_j > W A_i > W A_j \\ W A_i A_j &> W > W A_i > W A_j \\ W A_i A_j &> W A_i > W > W A_j \end{aligned} \quad (4)$$

655 Although we showed this for two single mutations in the wild type background, the same argu-  
 656 ments hold for any two sets of mutations in any background, since the succession of orderings is  
 657 independent of the rescalings of the fitness and concentration axes. To put it more precisely,  $W$ ,  $A_i$   
 658 and  $A_j$  are any three non-overlapping sets of mutations, where  $A_i$  and  $A_j$  are non-empty sets.

659 Next we use this to prove the accessibility property. Let  $\sigma$  have  $n$  mutations. It is sufficient to  
 660 prove that (i) any superset of  $\sigma$  with  $m$  or fewer mutations is accessible from all its own supersets  
 661 with  $m$  or fewer mutations, for all  $m \geq n$  (the statement follows from the case  $m = L$ ); and that (ii)  
 662 any subset of  $\sigma$  with  $m'$  or more mutations is accessible from any of its own subsets with  $m'$  or more  
 663 mutations, for all  $m' \leq n$  (the statement corresponds to  $m' = 0$ ). We prove this by induction.

664 Firstly, we notice that the case  $m = n$  is trivial, since  $\sigma$  is of accessible from itself. For the case of  
 665 supersets, our base case is  $m = n + 1$ , and the assertion above holds because  $\sigma$  is a local fitness peak,  
 666 and therefore accessible from all its supersets with  $n + 1$  mutations, which are of course accessible  
 667 from themselves.

668 Now we prove the induction step. Assume that all supersets of  $\sigma$  that have  $m$  or fewer mutations  
 669 (where  $m \geq n$ ) are accessible from all their supersets with  $m$  or fewer mutations. Consider a superset  
 670  $\Sigma$  of  $\sigma$  with  $m$  mutations, and denote it by  $\Sigma = \sigma A$ , where  $A$  is the set of mutations in  $\Sigma$  not present  
 671 in  $\sigma$ . By assumption,  $\sigma$  is accessible from  $\Sigma$ . In the following, we use the notation  $\sigma_1 > \sigma_2$  to indicate  
 672 that a genotype  $\sigma_1$  is fitter than a genotype  $\sigma_2$  (we use the " $<$ " and " $=$ " signs in a similar way).  
 673 Therefore, we have  $\sigma > \Sigma = \sigma A$ .

674 Now consider any superset of  $\Sigma$  with  $m + 1$  mutations, where the additional mutation not  
 675 contained in  $\Sigma$  is denoted  $B$ . Then this superset can be denoted by  $\Sigma B = \sigma A B$ . We must have  
 676  $\sigma > \sigma B$  since  $\sigma$  is a local fitness peak. We now have the relation  $\sigma > \sigma A, \sigma B$ . Therefore we must have  
 677  $\sigma A B < \sigma A, \sigma B$ , for otherwise we violate the ordering condition. Now since  $\Sigma B = \sigma A B < \sigma A = \Sigma$ ,  $\Sigma$   
 678 must be accessible from  $\Sigma B$ , proving that any superset with  $m$  mutations is accessible from any of  
 679 its supersets with  $m + 1$  mutations. This completes the proof of the induction step.

680 The proof for the case of subsets is essentially the same, utilizing the symmetry between the  
 681 wild type and the double mutant in the ordering condition.

682 The accessibility property follows entirely from the ordering condition, and hence any landscape  
 683 that obeys the ordering condition will obey the theorem. The ordering condition follows from  
 684  $X_{W,W_{A_i}} < X_{W_{A_j},W_{A_i A_j}}$ , as obtained in (3). However, this same inequality obtains under more general  
 685 conditions. To see this, let us define the null-fitness of the double mutant  $W_{A_i A_j}$  as  $r_{ij}$ , and the  
 686 resistance of the double mutant as  $m_{ij}$ . The dose-response curves of  $W$  and  $W_{A_j}$  intersect at  
 687  $X_{W,W_{A_j}} = x^*(r_j, m_j)$ , whereas the curves for  $W_{A_i}$  and  $W_{A_i A_j}$  intersect at

$$X_{W_{A_i},W_{A_i A_j}} = m_i x^*\left(\frac{r_{ij}}{r_i}, \frac{m_{ij}}{m_i}\right).$$

688 Now it is easy to show that  $x^*(r, m)$  is a decreasing function of both  $r$  and  $m$ . Therefore  $X_{W_{A_i},W_{A_i A_j}} >$   
 689  $X_{W,W_{A_j}}$  holds if  $r_{ij} \leq r_i r_j$  and  $m_{ij} \leq m_i m_j$ .

### 690 Number of local fitness peaks

691 When dealing with complex fitness landscapes with parameters that can vary across species and  
 692 environments, a useful strategy is to model the fitness effects as random variables that are chosen  
 693 from a probability distribution (*Kauffman and Levin, 1987; Szendro et al., 2013; Hwang et al., 2018*).  
 694 In the limit of large system size  $L$ , many properties emerge that are independent of the details of  
 695 the system. In practice, even relatively small system sizes are often approximated well by results  
 696 obtained in the asymptotic limit.

697 The mean number of peaks with  $n$  mutations in the tradeoff-induced landscapes is

$$K_n(x) = \binom{L}{n} Q_n(x),$$

698 where  $\binom{L}{n}$  is the total number of genotypes with  $n$  mutations, and  $Q_n(x)$  is the probability that  
 699 a genotype with  $n$  mutations is a fitness maximum at antibiotic concentration  $x$ . Then the total  
 700 number of peaks at  $x$  is  $\sum_n K_n(x)$ . Let the resistance of a genotype  $\sigma$  be  $M = \prod_{i=1}^n m_i$ , and likewise its  
 701 null-fitness be  $R = \prod_{i=1}^n r_i$ . The genotype  $\sigma$  is a local fitness maximum if it is fitter than all its subsets  
 702 with  $n - 1$  mutations and all its supersets with  $n + 1$  mutations.

703 To find the concentration at which the curves of  $\sigma$  and its neighboring genotypes intersect, we  
 704 start with the simplest case of the dose-response curves of the wild type and a single mutant  $(r, m)$ .  
 705 These curves intersect at the solution  $x^*(r, m)$  of  $w(x) = r w\left(\frac{x}{m}\right)$ , which is a decreasing function of  
 706  $r$  and  $m$ . The wild type is fitter than the single mutant when  $x > x^*(r, m)$ . Now the intersection of  
 707 the DR curves of a genotype  $\sigma$  with  $n$  mutations and a subset with  $n - 1$  mutations that lacks the  
 708 mutation  $(r_i, m_i)$  occurs at the solution of

$$w\left(\frac{x}{\left(\frac{M}{m_i}\right)}\right) = r_i w\left(\frac{x}{\left(\frac{M}{m_i}\right)m_i}\right)$$

709 which is read off as  $\frac{M}{m_i} x^*(r_i, m_i)$ . Likewise, the intersection of the DR curves of  $\sigma$  and a superset with  
 710  $n + 1$  mutations that contains the additional mutation  $(r_j, m_j)$  occurs at  $M x^*(r_j, m_j)$ . Therefore  $\sigma$  is a  
 711 fitness maximum if

$$\frac{x^*(r_i, m_i)}{m_i} < \frac{x}{M} < x^*(r_j, m_j) \quad (5)$$

712 for all  $i$  and  $j$  with  $1 \leq i < n$  and  $n < j \leq L$ . Alternatively,

$$\log m_i - \log x^*(r_i, m_i) > \log M - \log x > -\log x^*(r_j, m_j). \quad (6)$$

713 Let us consider the regime where  $L, n \gg 1$ . Then  $\log M \sim n \langle \log m \rangle$ ; if  $\log x$  is smaller than  $O(n)$ ,  
 714 it is clear that the second inequality is almost certainly satisfied whereas the probability of the  
 715 first inequality is vanishingly small. Both the probabilities are finite if  $\log x \sim n \langle \log m \rangle$ . Thus the  
 716 probability of  $\sigma$  being a fitness peak is maximized when  $\log x = \log(M) + \eta$ , where  $\eta \sim O(1)$  and  
 717 depends on the details of the distribution  $P(r, m)$ . Thus the mean number of fitness peaks with  $n$   
 718 mutations is maximal at  $x_{\max}(n)$  where to leading order  $\log x_{\max}(n) \sim n \langle \log m \rangle$ , independent of any  
 719 further details of the system.

720 The total number of genotypes with  $n$  mutations is  $\binom{L}{n}$ , and  $\log \binom{L}{n} \simeq LH(\rho)$ , where  $\rho = \frac{n}{L}$ , and  
 721 
$$H(\rho) = -[\rho \log \rho + (1 - \rho) \log(1 - \rho)]. \quad (7)$$

722 The mean number of fitness maxima can be found by multiplying this with  $Q_n$ . One may expect  $Q_n$   
 723 to be exponentially small in  $L$ , since a total of  $L$  inequalities (as indicated in (6)) need to be satisfied.  
 724 However, this is complicated by the fact that the probabilities of the inequalities being satisfied are  
 725 not independent. The correlations between the inequalities would depend on the distribution of  
 726  $P(r, m)$  and the dose-response curve. If the correlations are sufficiently weak, one might still expect  
 727 to find an exponential scaling in large  $L$ . To leading order  $\binom{L}{n}$  is itself exponential in  $L$ , and if the  
 728 probability that a genotype is a fitness peak is exponentially small in  $L$ , we expect the mean number  
 729 of peaks  $K_n$  to be exponential in  $L$  as well. This is supported by the scaling shown in the inset of  
 Figure 4A.

730 For the simulation results shown in the main text we chose a joint distribution of the form

$$P(r, m) = P(r)P(m|r) = 6r(1 - r)\left(m - \frac{1}{\sqrt{r}}\right)e^{-\left(m - \frac{1}{\sqrt{r}}\right)}. \quad (8)$$

731 The conditional distribution  $P(m|r)$  is a shifted gamma distribution. The shift ensures that the curves  
 732 of a background genotype and a mutant intersect.

### 733 Sign epistasis

734 Sign epistasis with respect to a certain mutation occurs when the mutation is beneficial in one  
 735 background but deleterious in another. We first show that any two distinct sets of mutations on  
 736 any genetic background display sign epistasis at some value of the scaled concentration  $x$ . Consider  
 737 a genetic background  $W$ , and two distinct sets of mutations  $A_1$  and  $A_2$  (which share no mutations  
 738 with each other or  $W$ ). At  $x = 0$  we have  $W > A_1, A_2$  and  $WA_1A_2 < WA_1, WA_2$ . As  $x$  increases,  $W$   
 739 must become less fit than either  $WA_1$  or  $WA_2$  before  $WA_1A_2$  becomes fitter than either of these (by  
 740 the ordering condition). Without loss of generality, let us assume that  $W$  becomes less fit than  $WA_1$   
 741 before it becomes less fit than  $WA_2$ . At this point, we must have  $W < WA_1$  and  $WA_2 > WA_1A_2$ .  
 742 This means that, in the wildtype background,  $A_1$  is beneficial in the absence of  $A_2$  but deleterious in  
 743 the presence of  $A_2$ , indicating pairwise sign epistasis.

744 To quantify the amount of sign epistasis for large  $L$  and  $n$ , we next ask for the number of  
 745 backgrounds  $n_b$  in which a mutation is beneficial at concentration  $x$ . If one considers only those  
 746 backgrounds that have  $n$  mutations, then  $n_b$  would depend both on  $n$  and  $x$ . In a statistical ensemble  
 747 of landscapes, one may compute the probability  $P_b$  that a mutation is beneficial in a background  
 748 with  $n$  mutations, and of course  $\langle n_b \rangle = P_b \binom{L}{n}$ . In the limit of large  $L$  and  $n$ ,  $P_b$  exhibits some universal  
 749 properties to leading order. When  $\log x > n \langle \log m \rangle$ , we are in the regime of high concentration relative  
 750 to  $n$ , and we expect a mutation to be beneficial. We find that to leading order  $P_b(\rho, x) = 1$ , with  
 751 corrections that are exponentially small in  $n$ . When  $\log x < n \langle \log m \rangle$ , we are at concentrations that  
 752 are too low to prefer additional mutations, and  $P_b$  is exponentially small in  $n$ . When  $\log x = n \langle \log m \rangle$ ,  
 753 we are at the threshold concentration where a new mutation becomes beneficial. Here we find that  
 754  $P_b \simeq \frac{1}{2}$ . For large  $L$  we therefore expect a steep transition from 0 to 1 as the concentration crosses  
 755 the threshold value (see inset of Figure 5).

756 Consider a mutation  $(r, m)$  in a background with  $n$  mutations  $(r_1, m_1), (r_2, m_2) \dots (r_n, m_n)$ . The mutation  
 757 is beneficial in this background if

$$m_1 m_2 \dots m_n x^*(r, m) < x \quad (9)$$

758 Taking logarithms, we have

$$-\log x^*(r, m) > \sum_{i=1}^n \log m_i - \log x. \quad (10)$$

759 Define  $\xi = \frac{\log x}{L}$  and  $\rho = \frac{n}{L}$ , and  $z = -\log x^*(r, m)$ . Then the above inequality becomes

$$\frac{z}{n} > \frac{1}{n} \sum_{i=1}^n \log m_i - \frac{\xi}{\rho}. \quad (11)$$

760 Let the distribution of  $z$  be  $P(z)$ , and let  $C_z(z) = \int_z^\infty P_z(x) dx$ . Define the random variable  $\omega =$   
 761  $\frac{1}{n} \sum_{i=1}^n (\log m_i - \frac{\xi}{\rho})$ , and denote its distribution  $P(\omega)$ . Then the probability that a mutation is beneficial  
 762 in a background with  $n$  mutations is

$$P_b(\rho, \xi) = \int_{-\infty}^{\infty} P(\omega) C_z(n\omega) d\omega \quad (12)$$

$$(13)$$

763 The mean number of backgrounds with  $n$  mutations in which a mutation is beneficial is  $n_b(\rho, \xi) =$   
 764  $P_b(\rho, \xi) \binom{L}{n}$ . Note that  $\langle \omega \rangle = \langle \mu \rangle - \frac{\xi}{\rho}$  where  $\mu = \log m$ . When  $n \gg 1$ ,  $C_z(n\omega) \simeq 1$  for  $\omega < 0$  and  $C_z(n\omega) \simeq 0$   
 765 for  $\omega > 0$ , with a sharp transition from 1 to 0 that happens within a region of width  $\sim O(1/n)$  of the  
 766 origin. Also for large  $n$ ,  $P(\omega)$  is sharply peaked around  $\langle \omega \rangle$  over a region of width  $O(1/\sqrt{n})$ .

767 When  $\langle \omega \rangle < 0$ ,  $C_z(n\omega) \simeq 1$  over this entire region, as observed before. Thus to leading order,  
 768  $P_b(\rho, \xi) = 1$ . The mean number of backgrounds in which a mutation is beneficial is  $n_b(\rho, \xi) =$   
 769  $P_b(\rho, \xi) \binom{L}{\rho L}$ .

$$n_b(\rho, \xi) \simeq \sqrt{\frac{2\pi}{L}} \frac{1}{\sqrt{\rho(1-\rho)}} e^{LH(\rho)} \quad (14)$$

770 where  $H(\rho)$  is defined in (7). Therefore

$$\log n_b \simeq LH(\rho) \quad (15)$$

771 to leading order.

772 When  $\langle \omega \rangle > 0$ , the dominant contribution to the integral in (12) comes from  $\omega \leq 0$ , since  $C_z(n\omega)$   
 773 quickly drops from 1 to zero for  $\omega > 0$ . Further, since  $C_z(n\omega) \simeq 1$  for  $\omega < 0$  (except for a region of width  
 774  $O(1/n)$  around  $\omega = 0$ , as observed before), we can approximate  $\log P_b(\rho, \xi)$  simply by the probability  
 775 that  $\omega < 0$ . Then

$$\log P_b(\rho, \xi) \simeq -nI\left(-\frac{\xi}{\rho}\right)$$

776 where  $I$  is the large deviation function of  $-\mu$ , and

$$\log n_b(\rho, \xi) \simeq L\left[H(\rho) - \rho I\left(-\frac{\xi}{\rho}\right)\right].$$

777 This implies that  $n_b$  is reduced by a factor that is exponentially small in  $L$  compared to (15)), and  
 778 therefore the fraction of backgrounds in which a mutation is beneficial is very small.

779 Finally, when  $\langle \omega \rangle = 0$ , i.e.  $\xi = \frac{n}{L} \langle \mu \rangle$ ,  $P(\omega)$  is centered at the origin and decays over a width  $O(1/\sqrt{n})$ .  
 780 For  $\omega > 0$ ,  $C_z(n\omega)$  is 0 except over a much smaller width  $O(1/n)$  to the right of the origin, whereas  
 781 for  $\omega \leq 0$ , it is 1 except for a small region of width  $O(1/n)$  left of the origin. Thus the dominant  
 782 contribution to the integral in (12) comes from  $\omega \leq 0$ , and as before,  $P_b$  can be approximated by the  
 783 probability  $\omega \leq 0$ . Due to the central limit theorem,  $P(\omega)$  is approximately Gaussian and therefore  
 784 symmetric around  $\omega = 0$ , and therefore  $P_b \simeq \frac{1}{2}$ . Consequently, we should have

$$n_b(\rho, \xi) \simeq \frac{1}{2} \sqrt{\frac{2\pi}{L}} \frac{1}{\sqrt{\rho(1-\rho)}} e^{LH(\rho)},$$

785 which is  $\frac{1}{2}$  times the total number of backgrounds given by (14). This proves that the concentration  
 786 where the mutation is beneficial in half of the backgrounds is given by  $\langle \omega \rangle = 0$  or  $\log x = n(\log m)$  for  
 787 large  $L$  and  $n$ .

788 **Epistasis in null-fitness and MIC for *E. coli* in the presence of ciprofloxacin**

789 Primary data shown in Table 1 were obtained from *Marcusson et al. (2009)*. In the third and  
 790 fifth columns, the errors in the  $\log(x)$  are calculated as  $\frac{|\Delta x|}{x}$ , where  $|\Delta x|$  are the standard error as  
 791 calculated from the standard deviations reported in the paper. The errors in columns four and  
 792 six were estimated as  $\sum_i \frac{|\Delta x_i|}{x_i}$  where the sum is over the mutations present in the combinatorial  
 793 mutants. The detectable cases of epistasis are marked in blue. Negative epistasis is found in all  
 794 these cases. Also, all the cases with epistasis correspond to two or more mutations that affect the  
 795 same chemical pathways.

Strain	String	log null-fitness	Non-epistatic	log MIC	Non-epistatic
MG1655	00000	0.00 (± .004)	NA	0.00 (± .35)	NA
LM378	10000	0.01 (± .016)	NA	3.17 (± .70)	NA
LM534	01000	-0.01 (± .018)	NA	2.75 (± .70)	NA
LM202	00010	-0.19 (± .020)	NA	0.69 (± .70)	NA
LM351	00001	-0.094 (± .014)	NA	1.08 (± .70)	NA
LM625	11000	-0.030 (± .011)	0.0 (± .038)	<b>3.17 (± .70)</b>	<b>5.92 (± 1.1)</b>
LM421	10010	-0.15 (± .019)	-0.18 (± .040)	4.13 (± .70)	3.56 (± 1.1)
LM647	10001	-0.051 (± .013)	-0.084 (± .034)	3.44 (± .70)	4.65 (± 1.1)
LM538	01010	-0.19 (± .020)	-0.20 (± .042)	4.13 (± .70)	3.46 (± 1.1)
LM592	01001	-0.083 (± .015)	-0.10 (± .036)	3.16 (± .70)	3.83 (± 1.1)
LM367	00011	-0.20 (± .026)	-0.28 (± .038)	2.06 (± .70)	1.77 (± 1.1)
LM695	11010	-0.24 (± .017)	-0.19 (± .058)	<b>3.85 (± .70)</b>	<b>6.61 (± 1.1)</b>
LM691	11001	-0.073 (± .013)	-0.094 (± .052)	<b>3.85 (± .70)</b>	<b>7.00 (± 1.4)</b>
LM709	10011	-0.24 (± .027)	-0.274 (± .054)	4.54 (± .70)	4.94 (± 1.4)
LM595	01011	<b>-0.51 (± .051)</b>	<b>-0.294 (± .056)</b>	4.54 (± .70)	4.52 (± 1.4)
LM701	11011	<b>-0.42 (± .037)</b>	<b>-0.284 (± .072)</b>	<b>4.83 (± .70)</b>	<b>7.69 (± 1.8)</b>

**Table 1.** The names of the strains and values of null-fitness (in competition assays with the wild type) in the third column and MIC (of ciprofloxacin) in the fifth column are obtained from *Marcusson et al. (2009)*. The binary strings represent the same genotypes as given in the caption of Figure 2. The values in parentheses are error estimates. The fourth and sixth columns are respectively the null-fitness and MIC values expected in the absence of epistasis. NA denotes the cases where this is not applicable.

## References

- 796  
797 Alexander, H. K. and MacLean, C. (2018). Stochastic bacterial population dynamics prevent the emergence of  
798 antibiotic resistance within the mutant selection window. *bioRxiv*, page 458547.
- 799 Andersson, D. I. and Hughes, D. (2010). Antibiotic resistance and its cost: is it possible to reverse resistance?  
800 *Nature Reviews Microbiology*, 8(4):260.
- 801 Andersson, D. I. and Hughes, D. (2014). Microbiological effects of sublethal levels of antibiotics. *Nature Reviews*  
802 *Microbiology*, 12:465–478.
- 803 Bank, C., Matuszewski, S., Hietpas, R. T., and Jensen, J. D. (2016). On the (un)predictability of a large intragenic  
804 fitness landscape. *Proc. Natl. Acad. Sci. USA*, 113:14085–14090.
- 805 Blanquart, F. and Bataillon, T. (2016). Epistasis and the structure of fitness landscapes: Are experimental fitness  
806 landscapes compatible with fisher's geometric model? *Genetics*, 203(2):847–862.
- 807 Brown, K. M., Costanzo, M. S., Xu, W., Roy, S., Lozovsky, E. R., and Hartl, D. L. (2010). Compensatory mutations  
808 restore fitness during the evolution of dihydrofolate reductase. *Mol. Biol. Evol.*, 27(12):2682–2690.
- 809 Chevereau, G., Dravecká, M., Batur, T., Guvenek, A., Ayhan, D. H., Toprak, E., and Bollenbach, T. (2015). Quantifying  
810 the determinants of evolutionary dynamics leading to drug resistance. *PLOS Biology*, 13:e1002299.
- 811 Chou, H.-H., Chiu, H.-C., Delaney, N. F., Segrè, D., and Marx, C. J. (2011). Diminishing returns epistasis among  
812 beneficial mutations decelerates adaptation. *Science*, 332:1190–1192.
- 813 Crona, K. (2020). Rank orders and signed interactions in evolutionary biology. *eLife*, 9:e51004.
- 814 Crona, K., Gavryushkin, A., Greene, D., and Beerenwinkel, N. (2017). Inferring genetic interactions from compara-  
815 tive fitness data. *eLife*, 6:e28629.
- 816 Crona, K., Greene, D., and Barlow, M. (2013). The peaks and geometry of fitness landscapes. *Journal of Theoretical*  
817 *Biology*, 318:1–10.
- 818 de Visser, J. A. G. M. and Krug, J. (2014). Empirical fitness landscapes and the predictability of evolution. *Nature*  
819 *Reviews Genetics*, 15(7):480.
- 820 de Visser, J. A. G. M., Park, S.-C., and Krug, J. (2009). Exploring the effect of sex on empirical fitness landscapes.  
821 *American Naturalist*, 174:S15–S30.
- 822 de Vos, M. G. J., Schoustra, S. E., and de Visser, J. A. G. M. (2018). Ecology dictates evolution? About the  
823 importance of genetic and ecological constraints in adaptation. *Europhysics Letters*, 122:58002.
- 824 DePristo, M. A., Hartl, D. L., and Weinreich, D. M. (2007). Mutational reversions during adaptive protein evolution.  
825 *Molecular biology and evolution*, 24(8):1608–1610.
- 826 Domingo, J., Diss, G., and Lehner, B. (2018). Pairwise and higher-order genetic interactions during the evolution  
827 of a trna. *Nature*, 558:117–121.
- 828 Drlica, K., Hiasa, H., Kerns, R., Malik, M., Mustaev, A., and Zhao, X. (2009). Quinolones: action and resistance  
829 updated. *Current topics in medicinal chemistry*, 9(11):981–998.
- 830 Durão, P., Balbontín, R., and Gordo, I. (2018). Evolutionary mechanisms shaping the maintenance of antibiotic  
831 resistance. *Trends in microbiology*, 26(8):677–691.
- 832 Ferretti, L., Schmiegelt, B., Weinreich, D., Yamauchi, A., Kobayashi, Y., Tajima, F., and Achaz, G. (2016). Measuring  
833 epistasis in fitness landscapes: the correlation of fitness effects of mutations. *Journal of theoretical biology*,  
834 396:132–143.
- 835 Flynn, K. M., Cooper, T. F., Moore, F. B.-G., and Cooper, V. S. (2013). The environment affects epistatic interactions  
836 to alter the topology of an empirical fitness landscape. *PLoS Genetics*, 9:e1003426.
- 837 Fragata, I., Blanckaert, A., Louro, M. A. D., Liberles, D. A., and Bank, C. (2019). Evolution in the light of fitness  
838 landscape theory. *Trends in Ecology & Evolution*, 34(1):69–82.
- 839 Franke, J., Klözer, A., de Visser, J. A. G. M., and Krug, J. (2011). Evolutionary accessibility of mutational pathways.  
840 *PLoS Computational Biology*, 7(8):e1002134.
- 841 Gillespie, J. H. (1984). Molecular evolution over the mutational landscape. *Evolution*, 38:1116–1129.

- 842 Gorter, F. A., Aarts, M. G. M., Zwaan, B. J., and de Visser, J. A. G. M. (2016). Dynamics of adaptation in experimental  
843 yeast populations exposed to gradual and abrupt change in heavy metal concentration. *American Naturalist*,  
844 187:110–119.
- 845 Gorter, F. A., Aarts, M. G. M., Zwaan, B. J., and de Visser, J. A. G. M. (2018). Local fitness landscapes predict yeast  
846 evolutionary dynamics in directionally changing environments. *Genetics*, 208:307–322.
- 847 Goulart, C. P., Mahmudi, M., Crona, K. A., Jacobs, S. D., Kallmann, M., Hall, B. G., Greene, D. C., and Barlow, M.  
848 (2013). Designing antibiotic cycling strategies by determining and understanding local adaptive landscapes.  
849 *PLoS ONE*, 8(2):e56040.
- 850 Gullberg, E., Cao, S., Berg, O. G., Ilbäck, C., Sandegren, L., Hughes, D., and Andersson, D. I. (2011). Selection of  
851 resistant bacteria at very low antibiotic concentrations. *PLoS pathogens*, 7(7):e1002158.
- 852 Hartl, D. L. (2014). What can we learn from fitness landscapes? *Current Opinion in Microbiology*, 21:51–57.
- 853 Hughes, D. and Andersson, D. I. (2017). Evolutionary trajectories to antibiotic resistance. *Annual Review of*  
854 *Microbiology*, 71:579–596.
- 855 Hwang, S., Schmiegel, B., Ferretti, L., and Krug, J. (2018). Universality classes of interaction structures for NK  
856 fitness landscapes. *Journal of Statistical Physics*, 172:226–278.
- 857 Kauffman, S. and Levin, S. (1987). Towards a general theory of adaptive walks on rugged landscapes. *Journal of*  
858 *theoretical Biology*, 128(1):11–45.
- 859 Kauffman, S. A. and Weinberger, E. D. (1989). The nk model of rugged fitness landscapes and its application to  
860 maturation of the immune response. *Journal of theoretical biology*, 141(2):211–245.
- 861 Kaznatcheev, A. (2019). Computational complexity as an ultimate constraint on evolution. *Genetics*, 212(1):245–  
862 265.
- 863 Khan, S., Beattie, T. K., and Knapp, C. W. (2017). The use of minimum selectable concentrations (mscs) for  
864 determining the selection of antimicrobial resistant bacteria. *Ecotoxicology*, 26(2):283–292.
- 865 Kingman, J. F. (1978). A simple model for the balance between selection and mutation. *Journal of Applied*  
866 *Probability*, 15(1):1–12.
- 867 Knopp, M. and Andersson, D. I. (2018). Predictable phenotypes of antibiotic resistance mutations. *mBio*,  
868 9(3):e00770–18.
- 869 Kolpin, D. W., Skopec, M., Meyer, M. T., Furlong, E. T., and Zaugg, S. D. (2004). Urban contribution of pharmaceuti-  
870 cals and other organic wastewater contaminants to streams during differing flow conditions. *Science of the*  
871 *Total Environment*, 328(1-3):119–130.
- 872 Kondrashov, D. A. and Kondrashov, F. A. (2015). Topological features of rugged fitness landscapes in sequence  
873 space. *Trends in Genetics*, 31(1):24–33.
- 874 Levin, B. R., Perrot, V., and Walker, N. (2000). Compensatory mutations, antibiotic resistance and the population  
875 genetics of adaptive evolution in bacteria. *Genetics*, 154(3):985–997.
- 876 Lobkovsky, A. E. and Koonin, E. V. (2012). Replaying the tape of life: quantification of the predictability of  
877 evolution. *Frontiers in Genetics*, 3:246.
- 878 Lozovsky, E. R., Chookajorn, T., Brown, K. M., Imwong, M., Shaw, P. J., Kamchonwongpaisan, S., Neafsey, D. E.,  
879 Weinreich, D. M., and Hartl, D. L. (2009). Stepwise acquisition of pyrimethamine resistance in the malaria  
880 parasite. *Proc. Natl. Acad. Sci. USA*, 106(29):12025–12030.
- 881 Marcusson, L. L., Frimodt-Møller, N., and Hughes, D. (2009). Interplay in the selection of fluoroquinolone  
882 resistance and bacterial fitness. *PLoS pathogens*, 5(8):e1000541.
- 883 Marrec, L. and Bitbol, A.-F. (2018). Quantifying the impact of a periodic presence of antimicrobial on resistance  
884 evolution in a homogeneous microbial population of fixed size. *Journal of Theoretical Biology*, 457:190–198.
- 885 Maynard Smith, J. (1970). Natural selection and the concept of a protein space. *Nature*, 225:563–564.
- 886 Melnyk, A. H., Wong, A., and Kassen, R. (2015). The fitness costs of antibiotic resistance mutations. *Evolutionary*  
887 *applications*, 8(3):273–283.

- 888 Mira, P. M., Meza, J. C., Nandipati, A., and Barlow, M. (2015). Adaptive landscapes of resistance genes change as  
889 antibiotic concentrations change. *Molecular biology and evolution*, 32(10):2707–2715.
- 890 Neidhart, J., Szendro, I. G., and Krug, J. (2014). Adaptation in tunably rugged fitness landscapes: the rough mount  
891 fuji model. *Genetics*, 198(2):699–721.
- 892 Ogbunugafor, C. B., Wylie, C. S., Diakite, I., Weinreich, D. M., and Hartl, D. L. (2016). Adaptive landscape by  
893 environment interactions dictate evolutionary dynamics in models of drug resistance. *PLoS computational  
894 biology*, 12(1):e1004710.
- 895 Ojkic, N., Lilja, E., Direito, S., Dawson, A., Allen, R. J., and Waclaw, B. (2019). A roadblock-and-kill model explains  
896 the action of the dna-targeting antibiotic ciprofloxacin. *bioRxiv*, page 791145.
- 897 Palmer, A. C., Toprak, E., Baym, M., Kim, S., Veres, A., Bershtein, S., and Kishony, R. (2015). Delayed commitment  
898 to evolutionary fate in antibiotic resistance fitness landscapes. *Nature communications*, 6(1):1–8.
- 899 Perelson, A. S. and Macken, C. A. (1995). Protein evolution on partially correlated landscapes. *Proceedings of the  
900 National Academy of Sciences*, 92(21):9657–9661.
- 901 Poelwijk, F. J., Kiviet, D. J., Weinreich, D. M., and Tans, S. J. (2007). Empirical fitness landscapes reveal accessible  
902 evolutionary paths. *Nature*, 445(7126):383.
- 903 Poelwijk, F. J., Tănase-Nicola, S., Kiviet, D. J., and Tans, S. J. (2011). Reciprocal sign epistasis is a necessary  
904 condition for multi-peaked fitness landscapes. *Journal of theoretical biology*, 272(1):141–144.
- 905 Pokusaeva, V. O., Usmanova, D. R., Putintseva, E. V., Espinar, L., Sarkisyan, K. S., Mishin, A. S., Bogatyreva, N. S.,  
906 Ivankov, D. N., Akopyan, A. V., Avvakumov, S. Y., Povolotskaya, I. S., Fillion, G. J., Carey, L. B., and Kondrashov,  
907 F. A. (2019). An experimental assay of the interactions of amino acids from orthologous sequences shaping a  
908 complex fitness landscape. *PLoS Genetics*, e1008079:15.
- 909 Regoes, R. R., Wiuff, C., Zappala, R. M., Garner, K. N., Baquero, F., and Levin, B. R. (2004). Pharmacodynamic  
910 functions: a multiparameter approach to the design of antibiotic treatment regimens. *Antimicrobial agents  
911 and chemotherapy*, 48(10):3670–3676.
- 912 Rehman, A., Patrick, W. M., and Lamont, I. L. (2019). Mechanisms of ciprofloxacin resistance in *Pseudomonas*  
913 *aeruginosa*: new approaches to an old problem. *Journal of Medical Microbiology*, 68:1–10.
- 914 Schenk, M. F., Szendro, I. G., Salverda, M. L. M., Krug, J., and de Visser, J. A. G. M. (2013). Patterns of epistasis  
915 between beneficial mutations in an antibiotic resistance gene. *Molecular biology and evolution*, 30(8):1779–  
916 1787.
- 917 Schmiegel, B. and Krug, J. (2014). Evolutionary accessibility of modular fitness landscapes. *Journal of Statistical  
918 Physics*, 154(1-2):334–355.
- 919 Schoustra, S., Hwang, S., Krug, J., and de Visser, J. A. G. M. (2016). Diminishing-returns epistasis among random  
920 beneficial mutations in a multicellular fungus. *Proc. Roy. Soc. B*, 283:20161376.
- 921 Stiffler, M. A., Hekstra, D. R., and Ranganathan, R. (2015). Evolvability as a function of purifying selection in *tem-1*  
922  $\beta$ -lactamase. *Cell*, 160(5):882–892.
- 923 Szendro, I. G., Schenk, M. F., Franke, J., Krug, J., and de Visser, J. A. G. M. (2013). Quantitative analyses of empirical  
924 fitness landscapes. *Journal of Statistical Mechanics: Theory and Experiment*, 2013(01):P01005.
- 925 Taute, K. M., Gude, S., Nghe, P., and Tans, S. J. (2014). Evolutionary constraints in variable environments, from  
926 proteins to networks. *Trends in Genetics*, 30:192–198.
- 927 Weinreich, D. M., Delaney, N. F., DePristo, M. A., and Hartl, D. L. (2006). Darwinian evolution can follow only very  
928 few mutational paths to fitter proteins. *Science*, 312:111–114.
- 929 Weinreich, D. M., Lan, Y., Wylie, C. S., and Heckendorn, R. B. (2013). Should evolutionary geneticists worry about  
930 higher-order epistasis? *Current opinion in genetics & development*, 23(6):700–707.
- 931 Weinreich, D. M., Watson, R. A., and Chao, L. (2005). Perspective: sign epistasis and genetic constraint on  
932 evolutionary trajectories. *Evolution*, 59(6):1165–1174.
- 933 Wistrand-Yuen, E., Knopp, M., Hjort, K., Koskiniemi, S., Berg, O. G., and Andersson, D. I. (2018). Evolution of  
934 high-level resistance during low-level antibiotic exposure. *Nature communications*, 9(1):1599.



- 935 Wood, K. B., Wood, K. C., Nishida, S., and Cluzel, P. (2014). Uncovering scaling laws to infer multidrug response of  
936 resistant microbes and cancer cells. *Cell Reports*, 6:1073–1084.
- 937 Wright, S. (1932). The roles of mutation, inbreeding, crossbreeding and selection in evolution. *Proc. 6th Int. Cong.*  
938 *Genet.*, 1:356–366.
- 939 Wu, N. C., Dai, L., Olson, C. A., Lloyd-Smith, J. O., and Sun, R. (2016). Adaptation in protein fitness landscapes is  
940 facilitated by indirect paths. *Elife*, 5:e16965.
- 941 Wünsche, A., Dinh, D. M., Satterwhite, R. S., Arenas, C. D., Stoebel, D. M., and Cooper, T. F. (2017). Diminishing-  
942 returns epistasis decreases adaptability along an evolutionary trajectory. *Nature Ecology & Evolution*, 1:0061.
- 943 Zagorski, M., Burda, Z., and Waclaw, B. (2016). Beyond the hypercube: Evolutionary accessibility of fitness  
944 landscapes with realistic mutational networks. *PLoS Computational Biology*, 12(12):e1005218.